

ANTIOXIDANT INTERVENTION WITH
MANGANESE(III)-SALOPHEN
IN THE SELENITE CATARACT MODEL
Implications For Cataract Disease

by

Kevin David Dell

Dissertation submitted to the Faculty of the
Virginia Polytechnic Institute and State University
in partial fulfillment of the requirements for the
degree of

DOCTOR OF PHILOSOPHY

in

Biochemistry

John L. Hess, Chairman

Eugene M. Gregory
David R. Bevan
Steven D. Holladay
Hara P. Misra

May 4, 1998
Blacksburg, Virginia

Key words: selenite, cataract, Mn-salophen, antioxidant, crystallins

Copyright ©1998, Kevin D. Dell

Antioxidant Intervention with Manganese(III)-Salophen in the Selenite Cataract Model: Implications for Cataract Disease

by

Kevin David Dell

Chairman: Dr. John Hess

(ABSTRACT)

Cataract disease affects millions of people worldwide. It is characterized by the accumulation of light-scattering bodies within the lens that reduce visual acuity. Cataracts are effectively treated surgically, but at great expense, costing Medicare \$3.4 billion in 1997. Development of an alternative therapy for this disease would provide medical and economic benefits.

We have investigated a novel antioxidant, the superoxide scavenger Mn(III)-salophen, as a therapeutic agent in the selenite cataract model. Mn(III)-salophen has been shown to protect *E. coli* colonies against oxidative stress but was untested in a eukaryotic system. A total dose of 300 $\mu\text{mol/kg}$, given IP in four equal 75 $\mu\text{mol/kg}$ doses spaced four hours apart, protects 75% of neonatal rats from nuclear cataract development five days after selenite injection.

Selenite is toxic through its reaction with the endogenous antioxidant glutathione (GSH). The reduction of selenite to selenide through an intermediate, selenodiglutathione (GSSeSG) leads to generation of superoxide radical, one of several toxic oxygen species that can damage the lens. Mn(III)-salophen causes an *in vitro* preservation of the lifetime of GSSeSG by interrupting the reduction of selenite. We have established that the reduction of GSSeSG to selenide does not use GSH as a reducing agent, but rather depends upon electrons generated in the earlier reduction of selenite to selenodiglutathione. These electrons can be intercepted by known one-electron scavengers, arresting the metabolism of GSSeSG.

Extensive proteolysis of lens crystallins and loss of calcium homeostasis occur in cataractous lenses from a rat treated with sodium selenite. The visual protection with Mn(III)-salophen is accompanied by a partial loss of the calcium homeostasis, a net increase in sodium, and calpain-mediated proteolysis of β -crystallins similar to lenses from animals treated with selenite alone. Although preservation of α -crystallins may contribute to the greater transparency in the protected lens, generalized β -crystallin proteolysis is insufficient for cataract formation.

From these experiments we propose that Mn(III)-salophen minimizes the oxidative stress imposed upon the cell by interfering with the metabolism of selenodiglutathione. This allows the cell to compensate for the loss of cation homeostasis and prevents aggregation of proteolyzed crystallins into cataracts.

Dedication

This work is dedicated to the memory of Lucien M. Geer. Lu was my teacher and friend, as such, he inspired me to never stop reaching and never stop dreaming. We were able to “bridge a gap across generations” and in so doing he passed on to me a love for learning and professional curiosity that drives me through the morass. Thank you Lu, for kind words and understanding throughout our friendship. I only wish you could be here in person as well as in spirit.

Acknowledgments

I would like to thank the members of my committee for countless hours of guidance and consultation: Dr. Misra, for his insight into radical metabolism and oxygen toxicity; Dr. Holladay, for his ability to see things from different perspectives and to look “outside the model”; Dr. Bevan, for his knowledge of toxicology and pharmacology in the use of a novel compound as well as his expertise in modeling; and Dr. Gregory, for the many meetings in which his probing questions opened whole new avenues of thought for me about the problem at hand.

Without my advisor, Dr. John Hess, I simply would not be here. His gentle guidance has allowed me to mature as a student. By allowing me the freedom to make mistakes, yet not letting me fall too far, he helped me transform into a scientist.

For invaluable technical assistance in the lab, I thank Youlin Tang. For financial support, I gratefully acknowledge the Virginia Tech Department of Biochemistry.

Finally, I would like to thank my family. To my mother and father, Susie and Bill Dell, thanks for the pride and confidence you have shown in me. It meant more than you could know. To my beloved wife, Lauren, you made it possible. Without you, all this would be meaningless.

TABLE OF CONTENTS

INTRODUCTION	1
1. REVIEW OF LITERATURE	3
ANATOMY AND PHYSIOLOGY OF THE LENS	3
CATARACT DISEASE.....	5
<i>Oxidative Stress and Cellular Defenses</i>	6
THE SELENITE MODEL.....	9
<i>Glutathione, Selenite, and Selenodiglutathione</i>	10
<i>Ion homeostasis and the importance of calcium</i>	11
RELEVANCE OF ANIMAL MODELS TO HUMAN CATARACT DISEASE	12
MN(III)-SALOPHEN.....	13
2. ADMINISTRATION OF MN(III)-SALOPHEN AND ITS PRESERVATION OF LENS TRANSPARENCY IN RATS	15
INTRODUCTION	15
MATERIALS AND METHODS.....	16
<i>Synthesis of Mn(III)-salophen</i>	16
<i>Maintenance of animals</i>	16
<i>Injection protocols</i>	16
<i>Removal of lenses</i>	17
<i>Toxicity Data</i>	17
RESULTS.....	17
<i>Preparation of Mn(III)-salophen</i>	17
<i>Administration and Short-term Toxicity of Mn(III)-salophen in vivo</i>	18
<i>Short-term visual effects (upon PSO and NC) of Mn(III)-salophen treatment</i>	18
<i>Long-Term Visual Effects</i>	22
<i>Cross-contamination</i>	23
DISCUSSION.....	24
<i>Visual Effects</i>	24
<i>Toxicity</i>	24
3. IN VITRO EFFECT OF MN(III)-SALOPHEN ON THE REACTION BETWEEN GLUTATHIONE AND SODIUM SELENITE	26
INTRODUCTION	26
MATERIALS AND METHODS.....	27
<i>Preparation of Mn(III)-salophen</i>	27
<i>HPLC Separation of Glutathione Oxidation Products by Selenite</i>	27
<i>Electron Paramagnetic Resonance (EPR) Studies</i>	28
<i>Molecular Modeling of Mn(III)-salophen</i>	28
RESULTS.....	28
<i>Oxidation of GSH by sodium selenite in vitro</i>	28
<i>Effect of Mn(III)-salophen and Mn(III)-acetate</i>	30
<i>Electron Paramagnetic Resonance (EPR) Studies</i>	33
<i>Effect of DMPO, MnSOD, and Catalase on GSH Oxidation by Selenite</i>	34
<i>Modeling of Mn(III)-salophen</i>	35
DISCUSSION.....	37
<i>Modeling of Mn(III)-salophen</i>	39
4. EFFECT OF IN VIVO SELENITE AND MN(III)-SALOPHEN ADMINISTRATION ON LENS ION HOMEOSTASIS AND LENS CRYSTALLIN PROTEOLYSIS	40

INTRODUCTION	40
MATERIALS AND METHODS.....	41
<i>Animal Care and Lens Removal</i>	41
<i>Analysis of Lens Proteins</i>	41
<i>Separation and Identification of Lens Crystallins</i>	41
<i>Glutathione content of lenses</i>	42
<i>Elemental analysis of lenses</i>	42
RESULTS.....	42
<i>Effect of Mn-Salophen and Selenite on Animal and Lens Weight</i>	42
<i>Lens Protein Quantities and Solubility in Buffer or Urea</i>	43
<i>Glutathione content of lenses</i>	48
<i>Elemental Analysis</i>	49
<i>Lens Water Content</i>	51
DISCUSSION.....	51
<i>Total Lens Protein and Nuclear / Cortical Distribution</i>	51
<i>Electrophoretic Studies</i>	52
<i>Calcium Homeostasis</i>	52
<i>Sodium/Potassium Homeostasis and Lens Hydration</i>	53
<i>Sulfur and Manganese Levels</i>	54
SUMMARY AND CONCLUSIONS.....	55
<i>Visual Protection by Mn(III)-salophen</i>	55
<i>In vitro GSH/Selenite Reaction</i>	56
<i>Calcium / Ion homeostasis</i>	57
<i>Crystallin Proteolysis</i>	57
<i>Model for in vivo protection with Mn(III)-salophen</i>	57
LITERATURE CITED	58
VITA.....	67

List of Figures

FIGURE 1-1 : STRUCTURE OF REDUCED GLUTATHIONE	8
FIGURE 1-2 : STRUCTURE OF SALOPHEN	14
FIGURE 2-1 : PSO GRADING SCALE	19
FIGURE 2-2 : MN-SALOPHEN PROTECTED LENSES AT 24 HOURS AFTER SELENITE	19
FIGURE 2-3 : LENSES 48 HOURS AFTER INJECTION	20
FIGURE 2-4 : NUCLEAR CATARACT GRADING SCALE	21
FIGURE 2-5 : MN-SALOPHEN PROTECTED LENSES AT 120 HOURS AFTER SELENITE	22
FIGURE 2-6 : LONG-TERM EFFECT OF MN-SALOPHEN/SELENITE TREATMENT	23
FIGURE 3-1 : SAMPLE CHROMATOGRAM OF GSH/SELENITE	27
FIGURE 3-2 : REDUCTION OF SELENITE BY GSH	30
FIGURE 3-3 : EFFECT OF MN-ACETATE AND MN-SALOPHEN ON REDUCTION OF SELENITE BY GSH	31
FIGURE 3-4 : REDUCTION OF SELENITE BY GSH (5:1 GSH:SELENITE)	32
FIGURE 3-5 : EPR CALIBRATION SIGNAL FROM HYDROXYL RADICAL	34
FIGURE 3-6 : ANTIOXIDANT EFFECT ON GSH/SELENITE REACTION	35
FIGURE 3-7 : ONE-SIDED STRUCTURE OF MN(III)-SALOPHEN	36
FIGURE 3-8 : TWO-SIDED STRUCTURE OF MN(III)-SALOPHEN	36
FIGURE 4-1 : ONE-DIMENSIONAL SDS-PAGE OF LENS PROTEINS AT 72 AND 120 HOURS AFTER SELENITE INJECTION	44
FIGURE 4-2 : TWO-DIMENSIONAL GELS OF TOTAL SOLUBLE PROTEIN FROM RAT LENS	45
FIGURE 4-3 : LENS NUCLEAR PROTEINS 120 HOURS AFTER SELENITE	46
FIGURE 4-4 : PROTEOLYTIC PROGRESSION IN MN-S/SELENITE-TREATED LENSES	48
FIGURE 4-5 : GLUTATHIONE LEVELS AFTER MN(III)-SALOPHEN TREATMENT	49

List of Tables

TABLE 2-1 : VISUAL PROTECTION FROM PSO / NC	20
TABLE 3-1 : REDUCTION OF SELENITE BY GLUTATHIONE	30
TABLE 3-2 : EFFECT OF 200 μ M MN-SALOPHEN UPON GSH/SELENITE REACTION	30
TABLE 3-3 : REDUCTION OF SELENITE BY GSH (WITH 200 μ M MN-ACETATE)	30
TABLE 3-4 : REDUCTION OF SELENITE BY GSH (5:1 GSH:SELENITE)	32
TABLE 3-5 : REDUCTION OF SELENITE BY GSH (5:2 GSH:SELENITE)	33
TABLE 3-6 : REDUCTION OF SELENITE BY GSH (WITH DMSO)	33
TABLE 4-1 : EFFECT OF SELENITE AND MN(III)-SALOPHEN UPON ANIMAL WEIGHT AND LENS WEIGHT 72 AND 120 HOURS AFTER SELENITE TREATMENT	43
TABLE 4-2 : TOTAL LENS PROTEIN AND RELATIVE SOLUBILITY 120 HOURS AFTER SELENITE INJECTION	43
TABLE 4-3 : ELEMENTAL ANALYSIS 72 HOURS AFTER SELENITE TREATMENT	50
TABLE 4-4 : ELEMENTAL ANALYSIS 120 HOURS AFTER SELENITE TREATMENT	50

List of Equations

EQUATION 1-1 : REDUCTION OF OXYGEN TO WATER	6
EQUATION 1-2 : DISMUTATION OF SUPEROXIDE	6
EQUATION 1-3 : THE METAL-CATALYZED HABER-WEISS REACTION	6
EQUATION 1-4 : REDUCTION OF SELENITE TO SELENODIGLUTATHIONE	10
EQUATION 1-5 : REDUCTION OF OXYGEN TO SUPEROXIDE BY HYDROGEN SELENIDE	11
EQUATION 3-1 : OXIDATION OF GSH BY SELENITE	26
EQUATION 3-2 : PROPOSED REACTION OF GSH WITH SELENITE	38
EQUATION 3-3 : BREAKDOWN OF GSSESG—PROPOSAL A	38
EQUATION 3-4 : BREAKDOWN OF GSSESG—PROPOSAL B	39

List of Abbreviations

ATP	Adenosine 5' Triphosphate
BSA	Bovine Serum Albumin
BSO	Buthione Sulfoximine
CAPS	3-(Cyclohexylamino)-1-propanesulfonic acid
DMPO	5,5-Dimethyl-1-pyrroline- <i>N</i> -oxide
DMSO	Dimethyl Sulfoxide
DNA	Deoxyribonucleic Acid
DTNB	5,5'-Dithio-bis-(2-Nitrobenzoic Acid)
DTPA	Diethylenetriamine Penta-acetic Acid
DTT	Dithiothreitol
EDTA	Ethylene Diamine Tetraacetic Acid
EGTA	Ethyleneglycol-bis-(β -amino-ethyl ether) N,N'-Tetra-acetic Acid
EPR	Electron Paramagnetic Resonance
GSH	Glutathione, Reduced Form
GSSG	Glutathione, Oxidized Form
HPLC	High Performance Liquid Chromatography
IP	Intraperitoneal
NC	Nuclear Cataract
PAGE	Polyacrylamide Gel Electrophoresis
PSO	Posterior Subcapsular Opacity
ROS	Reactive Oxygen Species
SDS	Sodium Dodecyl Sulfate
SOD	Superoxide Dismutase
SQ	Subcutaneous

INTRODUCTION

In cataract disease, a transparent lens progressively opacifies. In early stages, cataracts diminish visual acuity by scattering light as it passes through the lens, thereby prohibiting proper focusing onto the retina. Eventually, cataracts cause blindness by completely blocking light. At this writing, no pharmacological agent exists to reverse or treat cataract formation. Once cataracts have formed, surgical removal of the lens is the only means for improving vision.

Cataracts are a leading cause of blindness worldwide. Although cataract surgery is successful in most cases, it does have inherent risks and does not guarantee restored sight. Surgery also has a public policy downside: it is the largest line item expenditure for Medicare in the United States, totaling \$1.4 billion in 1994. Development of a medication that could retard or reverse cataract formation in humans would provide substantial long-term medical and economic benefits.

Cataracts have a variety of etiologies, including poisoning, irradiation, infection, genetic abnormality, and chronic diabetes.⁸⁵ However, the most common cause in humans is an accumulation of oxidative changes during aging.⁶⁸ Hence, we work toward the goal of developing a drug with relevance to age-related cataract disease. Discovery of compounds that inhibit cataractogenesis in an animal model contributes to the understanding of biochemical events causal to cataract formation. These compounds may also have potential for human pharmacological development. To seek a cure, we focus on traits common to most forms of cataracts. This approach has potential to benefit the most patients with the disease.

The process that transforms a clear, healthy lens into a cloudy, cataractous one is neither simple nor straightforward. The opaque lesions within the cataractous lens are caused by a disruption of the precise organization of the tissue that may incite formation of protein aggregates. The structural organization of the lens is disturbed by such changes as: loss of ionic homeostasis and resultant osmotic stress; activation of endogenous proteases with resultant proteolysis; oxidative stress with subsequent lipid peroxidation; and significant metabolic disturbances.

Our contribution to the long-term goals of understanding critical events in cataractogenesis and of pharmaceutical development has been to investigate the superoxide scavenger Mn(III)-salophen as a potential therapeutic antioxidant in the sodium selenite cataract model. Our specific objectives have been: to characterize how systemic treatment with Mn(III)-salophen affects the short and long-term morphology of selenite cataract; to examine how Mn(III)-salophen affects lens biochemistry, specifically its effects upon lens glutathione, calcium, sulfur, sodium, and potassium levels; to identify the effect of Mn(III)-salophen upon crystallin proteolysis and aggregation in the selenite cataract; to investigate any *in vitro* effect of Mn(III)-salophen upon the reaction between glutathione and selenite; and

finally, to model possible structures for Mn(III)-salophen. From the results of these experiments a mechanism is proposed by which Mn(III)-salophen protects against selenite-dependent cataractogenesis.

1. REVIEW OF LITERATURE

Anatomy and Physiology of the Lens

The lens is a flexible, transparent tissue located between the anterior and posterior chambers of the eye. Its flexibility allows a variable refractive index, enabling the lens to focus images of objects at different distances onto the retina. The suspensory ligaments change tension on the lens, stretching and flattening it to accommodate change in focal distance. The lens allows transmittance of greater than 95% of incident visible light,⁸⁵ which allows color vision across the complete visual spectrum as well as preventing damage from the energy of absorbed photons. The lens subsists as an essentially avascular tissue, thereby preventing the colorimetric absorption by hemoglobin in blood.

The mature lens consists of many layers of terminally differentiated fiber cells surrounded by a fibrous capsule. Beneath the capsule lies the anterior epithelium, a layer of competent cells from which the fiber cells are generated. The lens originates in the embryo as an outpouching of the head ectodermal layer, which becomes the rudimentary capsular epithelium.⁸⁵ During development, this layer of cells grows and develops into the functional lens by progressively laying down more fiber cells through mitosis and differentiation. Throughout life, growth occurs from the anterior epithelium, but there is no recycling of older tissue. Once their differentiation is complete, the fiber cells lose most of their organelles to minimize light scattering. These cells are dependent upon nutrient flow via diffusion from the aqueous humor to the vitreous humor mediated by the competent epithelium. As with all organic tissues, the lens is alive and metabolizing, but at a very low level in the nucleus—as close to stasis as living tissue will allow.

While rigidity provides the optimum environment for transparency, immobilizing the fiber cells and their macromolecules within is constrained by the need for lens flexibility. When the lens is considered as a large dynamic structure, both extracellular and intracellular factors contribute to this compromise between flexibility and transparency.

Extensive interdigitation of fiber cells semi-rigidly interlocks neighboring cells together. Each neighboring cell has a hexagonal cross-section, which allows tight, ordered packing. Hydration and osmotic pressures are tightly controlled with ion pumps and the strong fibrous capsule minimizes shear forces from stretching the lens. Extensive gap junctions exist to facilitate intercellular communication in the absence of vascular or nervous tissue. This communication minimizes differential responses to external stimuli that could create a refractile interface and scatter light.⁸⁵

Although half of the light refraction in the normal lens is due to lipid membranes, such refraction is minimized by the membranes' rigidity, caused by their very high cholesterol level. Maintenance of minimal protein-based refraction is possible through strict control of orientation of the crystallin

proteins to produce a glass-like or dense liquid state.³⁸ In order to optimize transparency, the fiber cells have differentiated to exclude organelles and consequently metabolism is very low.

The intact adult lens consists of 33% protein, 66% water, and trace amounts of lipid and carbohydrate.⁸⁵ Because of their very high concentration relative to other macromolecules, cytosolic proteins are of primary importance in maintaining lens transparency. Generation of a transparent lens depends upon maintaining strict control of the macromolecular orientation of these proteins within the cytosolic matrix.⁶

The major protein components in the lens are the three crystallin families, α -, β -, and γ -crystallin. The crystallin proteins are classified according to their gel chromatographic elution profile and can be grouped into structural and non-structural types.¹⁰⁴ The β - and γ -crystallins primarily have a structural function. The γ -crystallins are characteristic of a neonatal lens and occur in the earliest stage of tissue development. In these crystallins, multiple free sulfhydryl groups stabilize the tertiary structure; however, these groups are susceptible to an age-dependent altered, improper cross-linking. Two classes of γ -crystallins exist: γ_{DEF} , which predominates during the earliest development period and γ_{ABC} , which is synthesized later in the neonatal period.⁹³ This gradual transition in γ -crystallin expression is followed by a complete transition to β -crystallins as the animal matures, with only γ -crystallins being present in the nucleus of the adult animal. Therefore, the relative concentration of γ -crystallins decreases markedly with age as they are diluted by β -crystallins.¹⁴ As the lens ages, crystallins are post-translationally modified. Changes may include proteolysis or deamidation, which can cause formation of high-molecular-weight aggregates.¹⁰

Altered β -crystallins are more susceptible to aggregation and are typically insoluble. The α -crystallins are present to limit the chance of catastrophic denaturation, the third family of crystallins,. They are similar to the small heat shock protein family⁷ and serve as chaperones for their structural counterparts. This chaperone function protects against denaturation of other crystallins and preserves lens transparency. The α -crystallins protect against denaturation by stabilizing hydrophobic residues in early stages of protein unfolding.⁸⁶ Although originally thought to be lens-specific proteins, α -crystallins are present in many other tissues and can chaperone a variety of other proteins.⁴⁸

The ability of the α -crystallins to protect against aggregation is dependent upon many factors. Their activity may be affected by the level of glutathione and pantethine within the lens.²⁷ Deletions from its C-terminus drastically reduce the chaperone activity,² as does immobilization of the C-terminal end.⁹⁴ Deamidation results in changes to tertiary structure which allows sulfhydryl cross-linking, thereby deactivating the chaperone.⁷⁴ The ability of α -crystallin to function as a chaperone decreases with age, which may be related to formation of inactive high molecular weight aggregates.²⁴ It is not known whether inactive α -crystallins directly form aggregates or if the formation of aggregates inactivates α -crystallin.

The vulnerability of α -crystallin to modification that alters function of the protein is important because the lens depends upon these chaperones to maintain transparency in the dynamic lens environment. A loss of chaperone activity could predispose a lens to cataract formation by allowing denaturation of crystallins. Furthermore, a recent study demonstrates that chaperone proteins may have a stabilizing effect on cell membranes,⁹⁹ implying that the α -crystallins are critical for stability of lipid structure as well as protein.

Cataract Disease

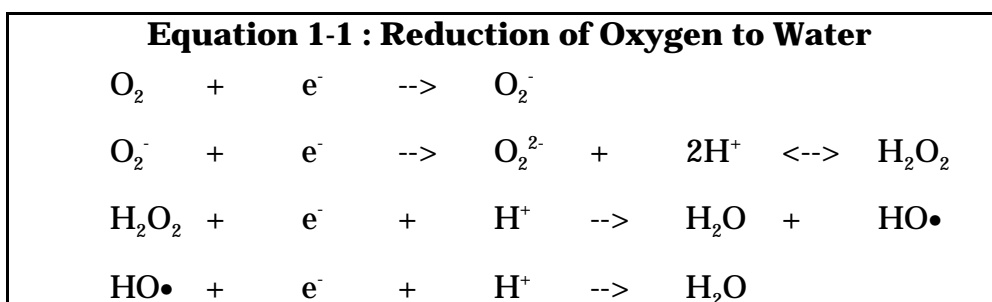
Because the normal lens is such a precisely ordered tissue, it is not surprising that any disturbance of the lens structure could cause it to lose transparency. A cataractous lens has regions of decreased transparency caused by discontinuities in refractive index and light scattering. Some cataracts have been associated with altered lens hydration, while others occur from localized disruptions in lens structure. Cataracts can be classified by their location within the lens as well as by demographic factors such as age of onset. They may be caused by a wide variety of insults to the lens, including trauma, infection, toxins, and oxidative stress.⁶⁸ Current data strongly support an oxidative mechanism contributing to human age-related cataracts, suggesting that antioxidant therapy could be a viable prophylaxis.^{5, 25.}

The direct cause of impaired vision is the presence of light scattering bodies, which have been identified as largely protein aggregates.⁶⁸ As the lens ages, it accumulates changes that include protein aggregation, covalent cross-linking, racemization of amino acids, increased pigmentation, and deamidation.¹⁰⁶ Over the past several years much has been learned about mammalian and avian lens development and fiber cell differentiation, leading to improved understanding of the formation, development, and maturation of the ocular lens. Age-related cataracts, however, are an acquired disease, not a developmental abnormality. Hence, we need to continue to learn about those changes that transform this highly organized transparent tissue to a lens that has a cataract.

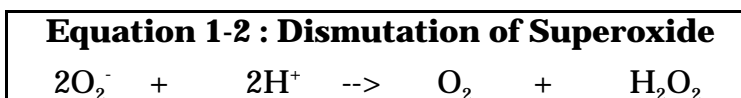
Realistic intervention strategies may be devised when the pathogenesis of cataract is defined in molecular terms. The prevention or delay of cataract formation has motivated several aspects of lens research. Several experimental cataract models based on putative oxidative stress are responsive to intervention by agents such as Mn(III)-desferral,⁹ pantethine,^{28, 29} methylthiazolidine-carboxylic acid (MTCA),⁵⁹ γ -glutamylcysteine ethyl ester,⁸³ ascorbate,⁴¹ deferoxamine,¹⁰² lipoic acid,⁷⁵ and vitamin E.⁶³ Each of these agents is expected to function through a unique mechanism that can provide information about particular aspects of cataract formation. Protection of visual transparency has been linked to the ability to prevent protein aggregation *in vitro*, as compounds which have been identified as visually protective in the selenite cataract model have been correlated according to their ability to raise the critical aggregation temperature of soluble protein (T_c) in lens extracts.⁶¹

Oxidative Stress and Cellular Defenses

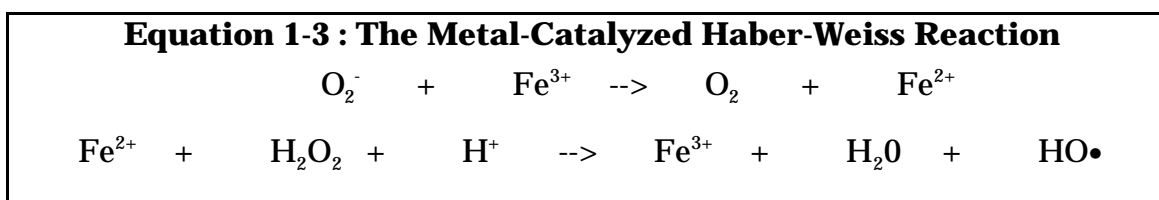
Dioxygen (O₂) has two unpaired electrons in its molecular antibonding π* orbitals. These electrons obey Hund's rule and are spin-parallel, which accounts for the paramagnetic behavior of oxygen gas. These parallel spin states require reduction through one-electron transfers,⁵³ or a collision of sufficient duration to allow spin inversion. The major species generated during the univalent reduction of dioxygen are superoxide, hydrogen peroxide, hydroxyl radical, and water. The stepwise reduction of dioxygen to water is outlined below:



Together, the three intermediate redox states of oxygen are classified as reactive oxygen species (ROS). Each poses unique challenges to a vulnerable cell. The first ROS, superoxide, can spontaneously dismutate to hydrogen peroxide and molecular oxygen; however, the rate is very slow and insignificant unless catalyzed: (Equation 1-2)



Hydrogen peroxide is toxic to the lens and is used to cause cataracts *in vitro*. It has been hypothesized to be a significant, if not primary, cause of oxidative damage related to aging in the eye.⁵² Superoxide can cause a number of deleterious biological effects, both directly and indirectly.⁴³ Superoxide can serve as either an oxidant or a reductant, both *in vitro* and *in vivo*,⁴⁵ which accounts for its direct action. A general review of the role of this chemistry in human disease is available.⁵⁵ An indirect mechanism for damage by superoxide is the generation of other ROS. The combination of superoxide and hydrogen peroxide in the presence of iron causes the catalytic generation of hydroxyl radical according to the Haber-Weiss reaction (Equation 1-3).



Hydroxyl radical can abstract an electron from almost any biomolecule, potentially causing severe physiological damage. DNA nucleosides can be directly damaged by hydroxyl radical,⁵⁸ as well as by other ROS,⁵⁴ and must be repaired before replication or transcription can occur. Abstraction of an electron can also initiate peroxidation of lipids in eukaryotic cells,¹⁷ with consequent loss of ion homeostasis and other destructive consequences.

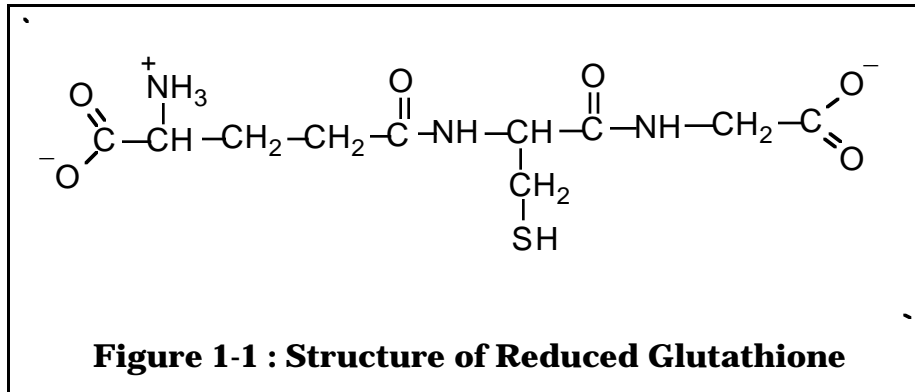
Coping with ROS is achieved through an integrated defense system. In a recent review, Fridovich identified four general mechanisms for managing oxidative stress: “{1} avoidance...{2} enzymatic removal of toxic oxygen species, {3} damage control by antioxidants...and {4} repair damage.”⁴⁴ Strategy one, avoidance, is particularly important in regions of the cell where reduction of oxygen is occurring. For example, in the mitochondria, tight control of these species is provided by cytochrome oxidase to minimize the exposure of reactive oxygen to the cell. For a utopic cell, such control would be sufficient, as oxygen would be present only when necessary. Unfortunately, as oxygen is ubiquitous in the environment, it is available to virtually all cellular processes. Therefore, it can react to form ROS whenever other species are present that undergo one-electron redox transfer, and thereby generate an oxidative stress.

In the lens, complete avoidance of oxidative stress is impossible, as photooxidation and active metabolism in the epithelial cells continuously generate radical species. Photooxidative energy is detoxified as pigments within the lens absorb this radiation, but this process generates the color changes seen in some cataracts.⁷¹ Repair of damage caused by ROS is possible in the competent epithelium, but very difficult in the differentiated fiber cells. Therefore, strategy two, enzymatic removal, and strategy three, antioxidant scavenging, are more important in the mammalian lens.

Strategy two, interception of ROS by enzymes, is achieved largely by superoxide dismutase (SOD), catalase, and glutathione peroxidase (GSHPx), each of which contributes to the general defense against oxidative stress.⁷⁸ SOD catalyzes the formation of hydrogen peroxide from superoxide (Equation 1-2) and catalase disproportionates two hydrogen peroxide molecules into two water molecules and molecular oxygen. GSHPx catalyzes the reduction of many organic peroxides to their organic hydroxide and water, through the oxidation of glutathione. GSHPx is particularly useful because of its lack of specificity for peroxide species.

Antioxidant enzymes in the lens catalyze removal of the toxic radical species, reducing the steady-state level of ROS.⁸⁷ Upon exposure to increased and sustained stress, the lens could increase the copy number of those enzymes. However, that strategy is generally ineffective within the adult lens nucleus, which has lost the capability for high levels of protein synthesis. Increasing copy number also does not protect against a short-term insult. A deluge of ROS that overwhelms the antioxidant enzymes must therefore be intercepted by radical scavengers.

Ascorbate, vitamin E, and glutathione are among the most important biological radical scavengers. Glutathione, in its reduced (GSH, Figure 1-1) and oxidized (GSSG) forms, plays a pivotal role in the intracellular antioxidant defense system. In addition to its role as a substrate for glutathione peroxidase, GSH is oxidized by superoxide to create a thiyl radical and hydrogen peroxide. The hydrogen peroxide can then be disproportionated by catalase or GSHPx. Part of a repair mechanism for a stressed cell involves removal of any irreversibly damaged molecules. This too is modulated to a certain extent by glutathione, as the ubiquitin-mediated proteolytic system is sensitive to glutathione redox states.⁶⁴ Maintenance of a supply of reduced glutathione is necessary for maintenance of cell homeostasis.



The reduction of GSSG to GSH is catalyzed by glutathione reductase, a flavoprotein that requires NADPH as an electron source. Many developing cells synthesize glutathione continuously and rely upon other tissues to recycle GSSG. Oxidized glutathione is not easily reduced or replaced in fiber cells, due to the low metabolic rate, leaving the nuclear region of the lens particularly susceptible to oxidative stress. Most cells can scavenge circulating GSH through the γ -glutamyl transpeptidase reaction,³⁹ but such recovery by lens is limited due to the low circulation. Therefore, direct oxidation of glutathione leaves lenses more susceptible to oxidative stress.³ When lenses are maintained in culture, they are dependent upon glutathione and an intact GSH redox cycle to detoxify low levels of H_2O_2 . Production of cataract by addition of an oxidant such as H_2O_2 proceeds with oxidation of GSH to GSSG with elevation of mixed disulfide (PSSG) levels.³⁰ Formation of protein-glutathione mixed disulfides contributes to cataract formation in the hydrogen peroxide induced cataract in rats.⁷³ Increased disulfide cross-linking is also a characteristic of age-related cataracts in humans.⁶⁸ If not reduced back to their original state, the mixed disulfides progress to protein crosslinks; however, the lens can recover from mixed disulfides alone if hydrogen peroxide is removed.¹⁰⁰

The Na^+/K^+ ATPase function may be dependent upon GSH levels.⁴⁹ In the absence of GSH reductase activity, much lower concentrations of hydrogen peroxide damage the Na^+/K^+ ATPase and ion homeostasis, although the Na^+/K^+ ATPase function may be restored over time.^{50, 51} The cell membrane sulfhydryl

groups are damaged by hydrogen peroxide, which may be responsible for loss of ion homeostasis.⁶⁰

Given the importance of glutathione in maintaining lens integrity, attempts have been made to augment its nominal level, thereby improving the cell's ability to withstand an oxidative stress. Glutathione levels can be raised *in vivo* by administration of cysteine pro-drugs;⁸⁸ however, elevating the lens glutathione level above that of a normal lens does not protect against high hydrogen peroxide levels.⁹⁶ Administering excess SOD in an attempt to prevent oxidative damage has met with only limited success, but low molecular weight antioxidant enzyme-mimics have been synthesized which could potentially be used for treatment against oxidative diseases.^{36, 46}

The Selenite Model

Selenium is a Group VIB metalloid which is chemically similar to sulfur and interacts with it. It is this interaction that makes selenium both essential and potentially toxic to the cell. Selenium can be integrated into the amino acid selenocysteine, which is necessary for several enzymes; therefore, selenium is nutritionally required in trace amounts. Animals with selenium deficiency are much more susceptible to oxidative insult; however, excess selenium is also toxic.¹⁰³ Selenium's antioxidant and chemoprotective activity is due to its required presence in the antioxidant enzyme glutathione peroxidase.²¹ Selenium is particularly toxic to proteins dependent on sulfhydryl redox states, because it can form adducts and directly damage proteins.⁶⁶ Subsequent changes in tertiary structure cause loss of protein function. Selenite also reacts with free reduced thiol pools such as glutathione and generates superoxide anion.⁶⁹

The toxicity of selenium has been well established for over 50 years.⁸¹ During early toxicity studies, sodium selenite was shown to cause nuclear cataracts in neonatal rats.¹⁹ Subcutaneous administration of 30 $\mu\text{mol/kg}$ sodium selenite in 20-30 g neonatal rats causes uniform, bilateral nuclear cataracts in all treated animals. The gross morphological course of cataract development in rats by this model has been well documented.⁹¹ After 24 hours, an opacity in the subcapsular region of the lens is noted, centering about the suture line at the extreme posterior aspect of the lens. This posterior subcapsular opacity (PSO) persists until approximately 72 hours after selenite treatment, when it is replaced by a consolidating nuclear cataract (NC). The NC is fully formed by 96 to 120 hours after selenite treatment. These effects can be manipulated to occur over a greater length of time in a chronic model of the disease.⁶³ Examination of the cataractous lesions present in the nuclear region of the lens reveals extensive crystallin proteolysis.

Significant biochemical changes occur in the lens following selenite treatment.¹⁹ Total glutathione levels in the selenite-treated lens decrease by 70% in the cortex and nucleus until well after cataract formation^{19, 80} and mitochondria show morphological damage.¹ Although the total GSH level decreases in the lenses of selenite-treated rats, the GSH/GSSG ratio does not appreciably shift, nor do mixed-protein disulfides increase. This total loss of

GSH is perplexing as it is not reproduced by simple *in vitro* incubation of selenite with GSH. Oxidized glutathione and GS- conjugates can be rapidly transported in an ATP-dependent manner out of cells,⁸⁴ and may contribute to the net GSH loss. Other changes after selenite treatment include an increase in pentose phosphate pathway activity, presumably to generate NADPH.¹⁹ Subsequently, free amino acid content increases,⁸⁰ and calcium homeostasis is lost.⁹¹

Another striking change seen in the lenses of selenite-treated animals is the temperature at which cold cataracts form. A cold cataract is a reversible phenomenon seen in the lenses from neonatal rats regardless of selenite treatment. As the lens cools from a physiological temperature of approximately 37° C, the nuclear region progressively becomes translucent, then finally opaque. This cataract formation occurs at roughly 30° C and is likely due to a temperature-dependent conformational change in α -crystallin that affects its ability to stabilize γ -crystallin. When an animal is treated with sodium selenite, the critical temperature is lowered, although the cataract does form and remains reversible. When combined with the observation that proteolysis of α -crystallin is seen on two dimensional electrophoresis, it is clear that the altered structure could affect the function of the chaperone crystallins.

Because of the rapid turnover of GSH within the cell, inhibition of its synthesis could provide another method for producing GSH depletion without direct oxidation and possible toxic byproducts. Buthionine sulfoximine (BSO) is a specific inhibitor of glutamylcysteine synthetase, the enzyme critical for GSH production within the cell. Administration of BSO to deplete GSH has been carried out, and although David and Shearer did not observe nuclear cataract in ten-day-old rats,³³ cataract has been observed in pre-weanling mice, indicating that GSH loss is sufficient for cataractogenesis.²² However, it is not yet clear in the selenite-induced cataract whether oxidative stress causes direct cell damage or whether the loss of GSH indirectly allows endogenous oxidative stress to cause the lens damage.

Glutathione, Selenite, and Selenodiglutathione

In vitro incubation of GSH with selenite produces a rapid oxidation of the GSH to GSSG with formation of selenodiglutathione, GSSeSG, according to the following reaction: ⁹⁵

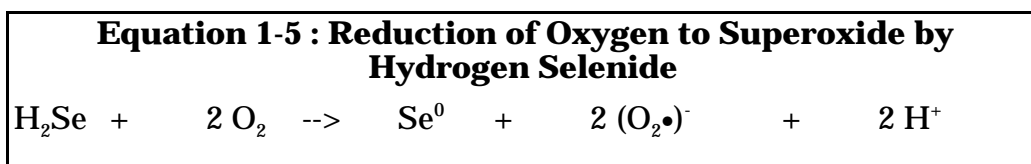
Equation 1-4 : Reduction of Selenite to Selenodiglutathione



Selenodiglutathione is one of a family of selenium-sulfur adducts called selenotrisulfides. A selenotrisulfide has the general structure RSSeSR and can be formed from many biological sulfur sources. Exchange of thiol between mixed selenotrisulfides and selenodiglutathione is possible⁸² and may further enhance the toxicity of selenodiglutathione. Selenodiglutathione is mutagenic in

*Salmonella typhimurium*⁶⁹ and is toxic to eucaryotic cells, inducing p53 and apoptosis⁷⁰ as well as inhibiting binding of transcription factor NF- κ B to DNA.⁶⁶ Due to the toxicity of this metabolite and the high level of glutathione present in the lens, the current prevailing hypothesis is that selenite is toxic *in vivo* through its interaction with endogenous GSH.

Selenodiglutathione is reduced to hydrogen selenide, H₂Se, which can reduce molecular oxygen to superoxide radical:⁹⁵



This formation of superoxide is thought to be the source of oxidative stress associated with selenite treatment. The autooxidation of thiols produces superoxide radical,⁷⁹ and *in vitro* selenite catalyzed oxidation of GSH to GSSG produces superoxide radical as well as the toxic intermediate selenodiglutathione (GSSeSG).⁹⁵ In the selenite-dependent cataract model, acceleration of cataract formation depends on oxidative stress.

With the depletion of lens GSH levels in the selenite model, the question arises of cause or effect of GSH loss on cataractogenesis. Since glutathione may form radical species to detoxify certain oxygen metabolites, it is possible that glutathionyl radicals are intermediate in damaging pathways. Glutathione will scavenge other radical species through a one-electron transfer, forming a (GS•) radical, which may be detected by spin-trapping with DMPO.^{56, 57, 89}

Ion homeostasis and the importance of calcium

Treatment with sodium selenite causes loss of Ca²⁺ homeostasis.²⁰ Calcium concentrations greater than 50 μ M activate the calcium-dependent protease *m*-calpain.³¹ *M*-calpain catalyzes amino-terminal cleavage of the structural β -crystallin proteins and carboxy-terminal cleavage of the α -crystallins within the lens.⁶⁵ These cleavages may cause conformational changes in the lens proteins resulting in formation of light scattering opacities.^{8, 92} Activation of calpain is self-limiting due to its autolytic activity.⁴ Although the effect of calcium appears to be greater on cortical homogenates than on nuclear homogenates,²⁶ the nucleus may also be affected through destabilization of the gap junctions in lens cells.⁷ This generalized disruption contributes to a cascade of damage throughout the tissue.

The specific changes within the cell leading to altered membrane function and loss of ion homeostasis are presently unclear, but they may result from oxidative damage to specific transporters or membrane lipids. The rate of Na⁺/Ca⁺⁺ exchange is lowered in membrane vesicles from the lenses of selenite-treated rats.¹⁰¹ Lipid peroxidation precedes nuclear opacification in human cataracts and products of peroxidation can be cataractogenic.⁵ The critical point at which oxidative insult becomes irreversible is unknown. While

proteolytic changes to the lens in the selenite-induced cataract have been well characterized,^{34, 65} the critical determinant of aggregation and formation of cataractous bodies has not. Many of the proteolytic changes to crystallins seen in selenite cataracts occur naturally as the lens matures, yet these lenses remain transparent.³¹ It is, therefore, of particular interest to determine whether specific protein changes are unique to cataract formation.

Relevance of Animal Models to Human Cataract Disease

Using human lenses to investigate causes of cataract formation has several important limitations. Because most cataractous lenses are from older individuals, it is difficult to isolate those changes in the lens which are related to aging but not necessarily cataract and vice versa. Whole lens studies are also difficult because ophthalmic surgeons now prefer to emulsify the lens before removal. Lenses are not removed until the benefit of surgery outweighs the risk; therefore, lenses with early cataract development are nearly impossible to obtain. Post-mortum changes in tissues make a cadaveric supply unreliable. Recently, sufficient advances have been made in recombinant DNA technology that individual human crystallins can be produced in native form;⁹⁸ however, such preparations are useful only for *in vitro* studies.

To conduct comprehensive studies, we must continue to develop and to study animal models that have properties related to cataract formation in human lens. When well characterized, such models may be used to screen for potentially therapeutic agents in preventing cataract or maintaining lens transparency. The value and relevance of a model requires that the protective agent be capable of affecting cellular events initiated by the causative agent.

Models involving cataract development in a mature lens are less suitable for evaluation of systemic antioxidants due to the lack of lenticular vascular supply. Of the animal models available, systemic administration of sodium selenite to preweanling rats is optimal for our goals because of its excellent reproducibility, rapid onset, low mortality, and suitable physiology. At 10-14 days old, rats retain the vascular bed perfusing the posterior aspect of the lens, which allows for systemic delivery of antioxidants. Because cataracts develop within five days, we may rapidly evaluate efficacy of antioxidant treatment. The low cost allows a large number of studies to be performed and a wide variety of antioxidant compounds to be screened.

When considering a developmental model such as the selenite model in rats, the question arises about the applicability of results across species lines. The selenite model differs from human cataracts in several important ways. The mixed disulfide level increases in human cataract disease,⁸⁵ but does not in selenite cataract,³³ implying a different result of GSH depletion. Human age-related cataracts occur in essentially static, fully differentiated fiber cells, while neonatal rats' cells continue to grow and retain some competence. The older human lens proteins have also undergone extensive post-translational modification prior to oxidative insult, while the neonatal rat lens proteins are much less modified. Finally, there is no evidence for calpain activation in human age-related cataract disease.

Those differences notwithstanding, the selenite cataract model is similar to human disease in several areas. Both types of cataract involve perturbations in ion homeostasis. Proteolysis is another common element of lens maturation in both species while protein aggregation is fundamental to the formation of cataract regardless of the model. It appears that protein aggregation may be a hallmark of cataract related to amyloid-like protein structures in various types of cataract.⁴² Recent work with confocal microscopy has identified abnormal lipid membrane structures in human cataractous lenses which are closely approximated with the selenite cataract model.¹⁵

Selenite, via free radicals, affects epithelial cell morphology and function, resulting in significant early metabolic responses to selenite treatment. The possible effect of free radicals directly on fiber cells is not well understood because this portion of the lens remains transparent through the process of nuclear cataract formation. The initial, transient posterior subcapsular opacity, however, does involve cortical fiber cells in the vicinity of the posterior suture. The potential action of free radicals on the nuclear fiber cells is of interest, since it is the nucleus of the lens that becomes greatly affected modified and is the locus of protein aggregates that cause nuclear cataract. Generally we lack knowledge about the sustained impact of free radicals on the cortical and nuclear fiber cells.

Mn(III)-salophen

Mn(III)-salophen is a Schiff base complex reported to scavenge superoxide⁷⁶ as well as disproportionate hydrogen peroxide.⁹⁰ It is formed by the complexation of Mn³⁺ with salophen (N, N'-Bis(salicylidene)-1,2-phenylenediamine, Figure 1-2) in a 1:1 ratio. Mn(III)-salophen enables the aerobic growth of SOD-deficient *E. coli* cultures on minimal media,⁷² but its action has not been characterized in an animal model. Because Mn(III)-salophen scavenges the toxic species reportedly generated in the selenite cataract model, it could potentially be used to affect the cataractogenic process *in vivo* when administered to selenite-treated rats. When compared to many other synthetic antioxidants, Mn(III)-salophen offers the advantage of being readily synthesized from inexpensive, commercially available components. The availability of Dr. E. M. Gregory for consultation in its use facilitated the development of a method for using Mn(III)-salophen in this experimental system and furthering our understanding of the mechanism of selenite action.

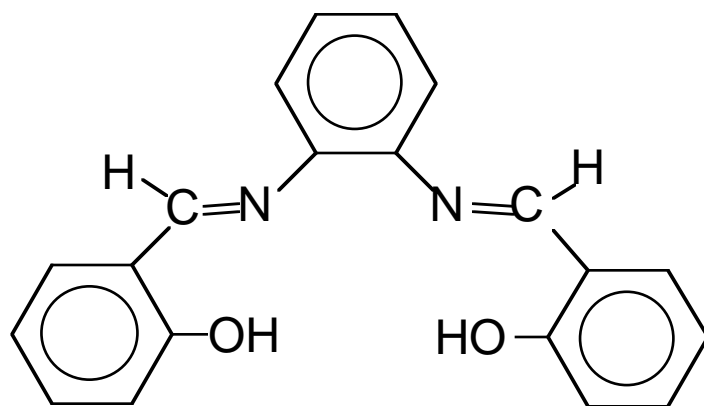


Figure 1-2 : Structure of Salophen

2. ADMINISTRATION OF Mn(III)-SALOPHEN AND ITS PRESERVATION OF LENS TRANSPARENCY IN RATS

Introduction

Reactive oxygen species (ROS) have been implicated as contributors to many human diseases, including diabetes mellitus, reperfusion injury, and cataracts. The three major ROS are the intermediate redox states between triplet oxygen and water: superoxide anion radical, peroxide anion, and hydroxyl radical. As a group, ROS interfere with normal metabolic chemistry and may perturb macromolecular structures; such perturbations include DNA cross-linking and lipid peroxidation. Although low levels of ROS are present in all aerobic organisms, elevated ROS may be caused by exposure to environmental oxygen or by failure of the endogenous antioxidant defense system. In cases where ROS lead either directly or indirectly to disease states, administration of antioxidants, either natural or synthetic, may be beneficial in treating the disease.

Of the reactive oxygen species, superoxide radical is of particular importance.⁴³ It is formed by a single electron adding to molecular oxygen, and can form other ROS by dismuting to hydrogen peroxide or by forming hydroxyl radical in the presence of hydrogen peroxide. Although it is regarded as a precursor to hydroxyl radical, the most toxic ROS, superoxide is individually toxic as well. Defense against superoxide is primarily in the form of superoxide dismutases that catalyze the formation of hydrogen peroxide from these radical ions. When endogenous SOD is insufficient to handle an overwhelming oxidative burst, it would be useful to administer a compound to augment SOD *in vivo*.

Although other intracellular metabolites such as glutathione can scavenge an electron from superoxide as well, there is interest in organic complexes of Mn that may detoxify superoxide anion.⁴⁶ Manganese (III)-salophen is a compound which has superoxide scavenging ability and possibly SOD-mimic activity.⁷² It has also been reported to disproportionate hydrogen peroxide. In mutant *E. coli* which were deficient in SOD and unable to tolerate an oxygen atmosphere, Mn(III)-salophen allowed normal growth, substituting for the absent SOD.⁷² As of this writing, it has not been described in a eukaryotic system.

In these experiments Mn(III)-salophen was administered to neonatal rats exposed to sodium selenite. Selenite oxidizes reduced glutathione (GSH) *in vitro* and generates superoxide. This oxidative stress results in bilateral nuclear cataracts within five days. In this study we have examined the effect of Mn(III)-salophen on rats treated with a cataractogenic dose of selenite.

Materials and Methods

Except where specifically noted, chemicals were purchased from Sigma Chemical Company (St. Louis, MO).

Synthesis of Mn(III)-salophen

Ethanol-based solutions of Mn(III)-salophen were prepared at concentrations of up to 40mM by dissolving commercial salophen (Aldrich 26,949-2) in absolute ethanol at pH 10. After the pH was reduced to ~5.5 with concentrated HCl, equimolar amounts of Mn(III)-acetate were added and the solution vigorously agitated. Once the solute was completely dissolved, the pH was increased to ~7.5 with concentrated sodium hydroxide. DMSO-based solutions of Mn(III)-salophen were prepared at concentrations up to 100mM by dissolving salophen and Mn(III)-acetate individually in ultrapure DMSO then mixing in equimolar proportions. Superoxide scavenging activity of Mn(III)-salophen was measured spectrophotometrically at 550 nm by inhibition of the superoxide-dependent reduction of cytochrome *c* in the xanthine/xanthine oxidase/cytochrome *c* assay.⁷⁷

Maintenance of animals

All protocols involving experimental animals were approved by the Animal Use and Care Committee of Virginia Tech and the University Veterinarian. Sprague-Dawley rat breeding pairs were obtained from Harlan Sprague-Dawley (Dublin, VA) and maintained in the university vivarium at 20-24 °C and 50 % relative humidity. Adults were fed Teklad 7004 breeder diet and distilled water *ad libidum*. Female rats produced an average of 6-8 usable litters during their lifetime. Litters were culled to twelve within four days of birth. Pre-weanling rats were kept with their parents and the pups were allowed to nurse without interference. Pups used in long-term studies were weaned after 21 days and maintained similarly to other adults, although segregated by gender to prevent breeding.

Injection protocols

The injection protocol was started on day 12 ± 2 of life (birth is day 0). All acute selenite model protocols began with pups injected subcutaneously (SQ) with sodium selenite at 30µmol/kg body weight, to be followed when appropriate by injection of the intervention agent or vehicle 45 min. ± 15 min. later. Animals were injected using a Hamilton gas tight slip-tip syringe attached to a 26 gauge 3/4" needle (Beckton-Dickenson & Co., Rutherford, NJ). Mn-salophen dosing started at two doses of 50 µmol/kg and was varied by dose, timing, vehicle, and route of administration until maximal effect was seen (see Results below). The final dosing sequence consisted of four intraperitoneal (IP) injections of 75 µmol/kg spaced four hours apart, beginning 1 hour after selenite injection. Solutions used for *in vivo* injection were mixed immediately prior to use. Controls to evaluate individual effects of Mn(III)-acetate and salophen were carried out substituting the synthetic component in place of

Mn(III)-salophen. Controls to rule out interference by the delivery vehicle alone were carried out by equivolume injections of ethanol or DMSO.

Removal of lenses

Animals were killed at 24-120 hours after selenite injection and their eyes examined for visible disturbances. Animals were weighed prior to the initial injection and just prior to being killed. Animals were decapitated and their eyes removed by incision at the lateral rectus muscle followed by separation of medial, dorsal, and ventral recti. The eye was lifted out of its socket and the optic nerve severed. The globe of the eye was opened by incision at the optic nerve root with a #11 scalpel followed by creation of a flap in the posterior sclera through which the lens was expelled. The lens was bathed in 0.9% sodium chloride at 37° C and cleaned of vitreous and aqueous debris under an Olympus dissecting microscope equipped with a model SZH-ILLD dark field below-stage illuminator. Lenses were transferred to fresh saline and photographed through the same microscope under dark or light field illumination to Ektachrome 200ASA slide film. For lenses from animals 24-48 hours after selenite injection, posterior subcapsular opacities were graded on a zero to four scale (with + and - gradations to yield an approximate ten point scale--See Figure 2-1). For animals 96-120 hours after selenite injection, NCs were graded on a four point scale (Figure 2-4). All lenses were compared with control animals from the same litter.

Toxicity Data

Animals from positive control, negative control, Mn-salophen only, and selenite & Mn-salophen groups were maintained into adulthood. These animals were handled similarly to the juvenile rats; however, they were killed by CO₂ asphyxiation prior to lens removal and necropsy. Gross tissue specimens were obtained and preserved for microscopic analysis. Acute toxicity was determined by any of several clinical signs: neurological impairment, poor motor control, muscle spasm, or loss of reflexes; local impairment, edema or necrosis; or systemic impairment, failure to thrive or death. Animals that died unexpectedly were necropsied by the university veterinarian.

Results

Our initial investigation of Mn(III)-salophen included experiments to synthesize the compound, determine its efficacy in scavenging superoxide, and examine its effect on *in vitro* and *in vivo* selenite-treated systems. These experiments were followed by preliminary trials of Mn(III)-salophen in neonatal rats.

Preparation of Mn(III)-salophen

Synthesis of Mn(III)-salophen was carried out as described above. Solutions of 40 mM could be prepared in ethanol; however, pH control was critical. Allowing the pH to exceed 8.0 resulted in a rapid precipitation of a muddy brown solute which would not redissolve if the pH were lowered. When

prepared in DMSO, a concentration of 100 mM could be obtained, and pH was no longer relevant. Regardless of solvent, our Mn(III)-salophen showed the characteristic increase in absorbance over the visible range 400-475 nm and was found to have 1.1 ± 0.1 unit of superoxide scavenging activity at a concentration of $0.67 \mu\text{M}$, in agreement with Liu and Gregory.⁷²

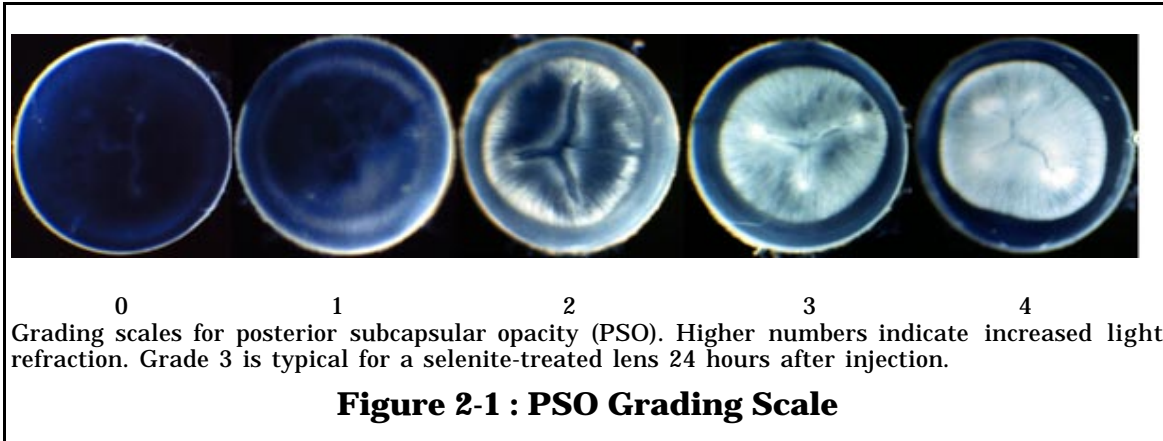
Administration and Short-term Toxicity of Mn(III)-salophen in vivo

Our initial low-dose Mn(III)-salophen protocol was extrapolated from the successful prevention of cataractogenesis in rabbits with Mn(III)-desferal pink-complex.⁹ These protocols were modified based upon the animals' systemic and lenticular response to the compound, titrating for visual protection with no toxic effects.

Attempts to increase the dosage beyond $50 \mu\text{mol/kg}$ every eight hours resulted in significant toxic effects, which the university veterinarian evaluated as being due to excess ethanol administration. In order to increase the dose of Mn(III)-salophen delivered within a minimum volume, the solvent was changed to DMSO which accommodated concentrations up to 100mM. Experiments to evaluate effects of Mn(III)-acetate or salophen were carried out by equimolar IP injection of the compound in place of Mn(III)-salophen. Controls to rule out interference by the delivery vehicle alone were carried out by equivolume injections of ethanol or DMSO.

Short-term visual effects (upon PSO and NC) of Mn(III)-salophen treatment

Selenite injection was followed by IP injections of 40 mM Mn(III)-salophen in ethanol ($50 \mu\text{mol/kg}$ body weight) at 30 minutes and 8.5 hours after selenite injection. Animals were killed at 24, 48, and 120 hours after selenite injection and their lenses examined for PSO or NC. Partially protected PSOs were grouped by visual patterns of the very small clusters of refractile swelling seen on the dissecting microscope as follows: stage 1 PSOs consisted of a posterior ring of refraction near the equator but not involving the sutures; stage 2 PSOs had extensions from the refractile ring down to the suture lines; and stage 3 PSOs also involved the area between the suture rings. Clear lenses were evaluated as stage 0, and any progression of the PSO from the superficial capsule into the deeper cortex of the lens was called stage 4 (Figure 2-1). Lenses with opacities of intermediate grades were designated with a +/- system.



Positive control animals had stage 3 bilateral PSOs 24 hours after selenite injection. Negative control animals had clear (stage 0) lenses at all times. Treatment with 100 $\mu\text{mol/kg}$ Mn(III)-salophen/EtOH solution in addition to selenite produced a spectrum of either fully or partially protected PSOs. Within this spectrum, protection was defined as having less than stage 2 in any particular lens. In the Mn(III)-salophen/EtOH treatment group, 75 % of animals treated were evaluated as having significant lens protection (Figure 2-2). Treatment with Mn(III)-acetate instead of Mn(III)-salophen protected 18% of animals from PSO formation. Salophen did not protect animals against PSO formation. (Table 2-1)

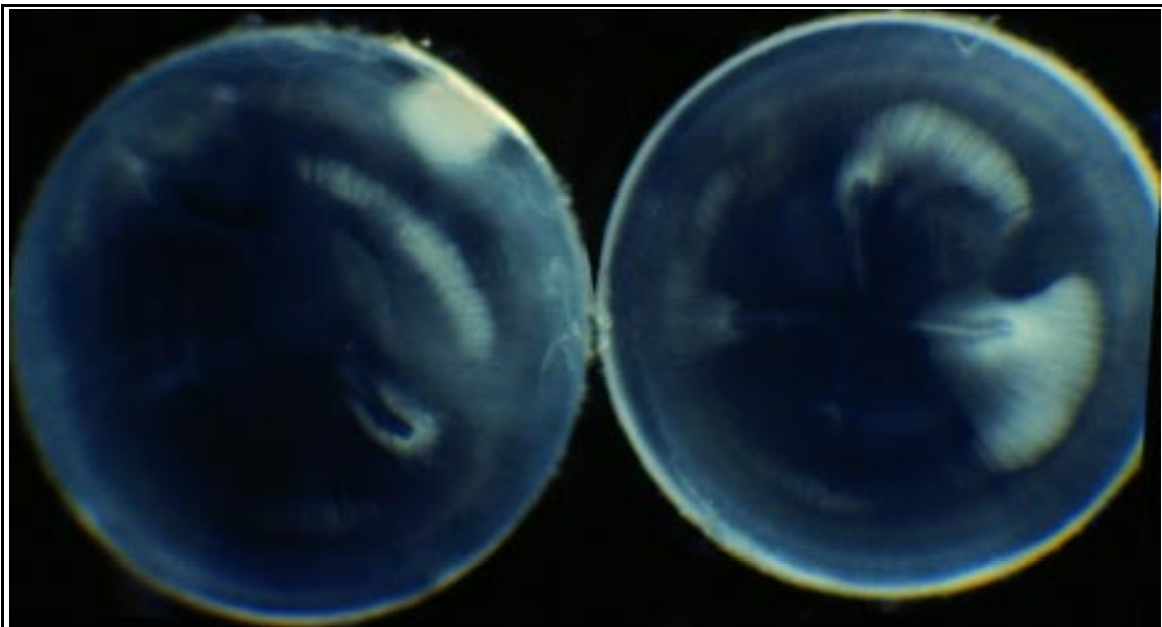


Figure 2-2 : Mn-Salophen Protected Lenses at 24 hours after Selenite

Table 2-1 : Visual Protection from PSO / NC

Protected Lenses under various treatments. Vehicle and synthetic component controls protection data was based on a minimum of 6 observations. Low and high dose Mn(III)-salophen treatment data were based on a minimum of 12 observations, with a variation is $\pm 5\%$.

	24 hours ¹	48 hours ¹	96-120 ² hours
Vehicle (EtOH or DMSO, 1.5 ml kg ⁻¹ day ⁻¹)	0	-- ³	0
Mn(III)-acetate⁴	18	25	--
Salophen⁴	0	--	--
Mn(III)-salophen⁴	75	50	33
Mn(III)-salophen (300 μ mol kg ⁻¹ day ⁻¹ in DMSO)	33	50	75

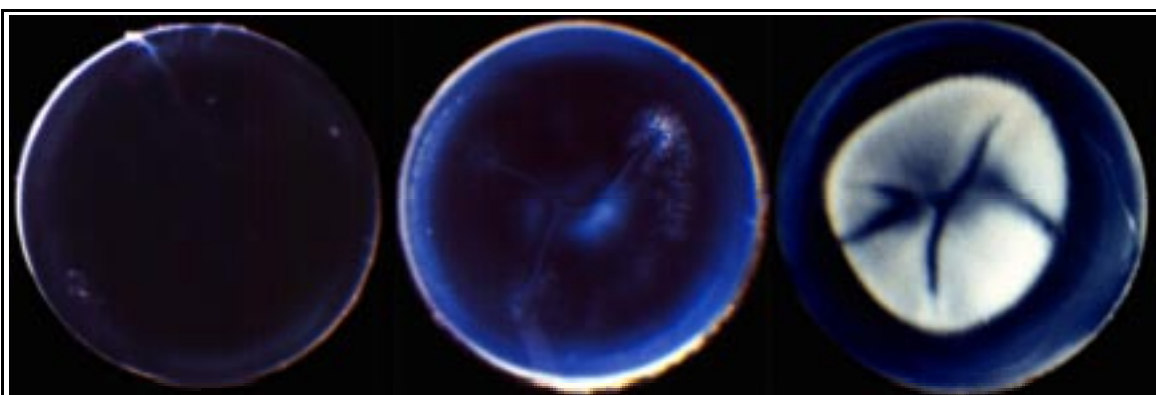
¹24-48 hour lenses are considered protected if PSO is less than stage 2.

²96-120 hour Lenses are considered protected if NC is minimal or less.

³Not Determined

⁴100 μ mol kg⁻¹ day⁻¹ in EtOH

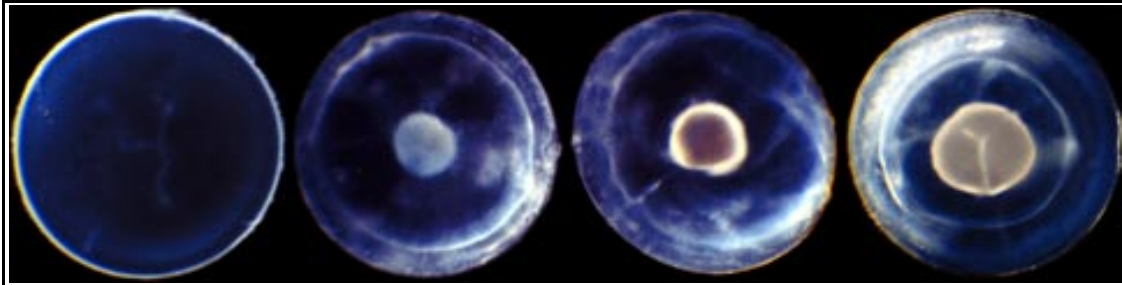
Antioxidant dosing protocols were extended to two days of treatment by either repeating the initial day's treatment (2 injections of 50 μ mol/kg eight hours apart) or by giving a total of six injections of 50 μ mol/kg every 8 hours, starting 30 minutes after selenite injection. Animals were killed 48 hours after selenite injection to evaluate PSO formation in their lenses. This dose protected 50% of treated animals from PSO formation.



Left to right: lenses from (-) controls, selenite and Mn(III)-salophen, and (+) controls. Pictures were taken under a dark-field microscope and scanned.

Figure 2-3 : Lenses 48 hours after Injection

For lenses obtained 96 or 120 hours after selenite injection, visual protection was determined based upon the amount of nuclear opacity. The nuclear regions were evaluated as either transparent, partially cataractous, or completely cataractous. Partially cataractous lenses were translucent or opaque but had insufficient density to appear colored under darkfield microscopy. Completely cataractous lesions were also evaluated for size, resulting in a final four point grading scale for NC (Figure 2-4) For a lens to be considered protected, it could be clear or partially cataractous. All protected lenses were compared with positive and negative controls from the same litter.



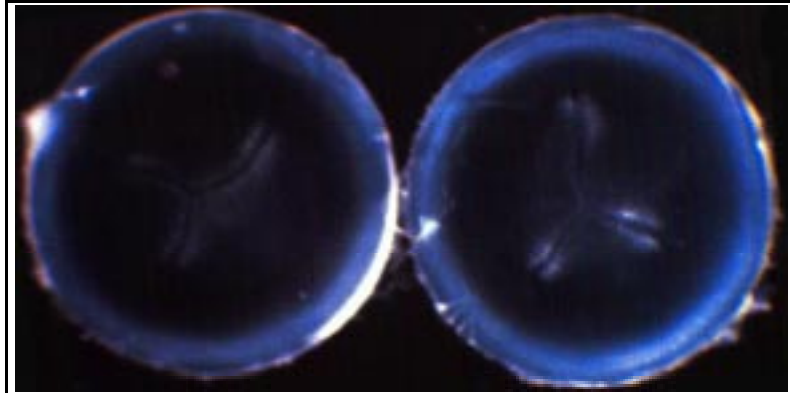
Grading scales for nuclear cataract. From left to right: none, minimal, small, and full opacities respectively. Full opacities were seen in unprotected lenses 96-120 hours after selenite treatment.

Figure 2-4 : Nuclear Cataract Grading Scale

High dose Mn(III)-salophen injections were started between 30 minutes and 2 hours after selenite injection, with a second injection of Mn(III)-salophen following 8 hours after the first. High doses of Mn(III)-salophen in DMSO ranged from 50 to 150 $\mu\text{mol/kg}$.

By moving the administration of Mn(III)-salophen to 2 and 10 hours after selenite, 2 doses of 150 $\mu\text{mol/kg}$ provided excellent protection in 66% of lenses from treated animals. Further adjustment to 4 doses of 75 $\mu\text{mol/kg}$ at 1, 5, 9, and 13 hours after selenite administration provided the best protection, with 70-80% of treated lenses showing no nuclear opacity at 120 hours (Figure 2-5 and Table 2-1). The vehicle control group (DMSO and selenite) had no visual protection from cataract formation.

Changing the route of administration of Mn(III)-salophen to subcutaneous from intraperitoneal decreased the protection from NC to less than 25% (Data not shown). Although the selenite cataract model has an administration window of 10-14 days, we found Mn(III)-salophen protection to be reproducible only if the animals weighed less than 25 grams at the time of selenite injection, which limited experiments to animals 10-12 days old.

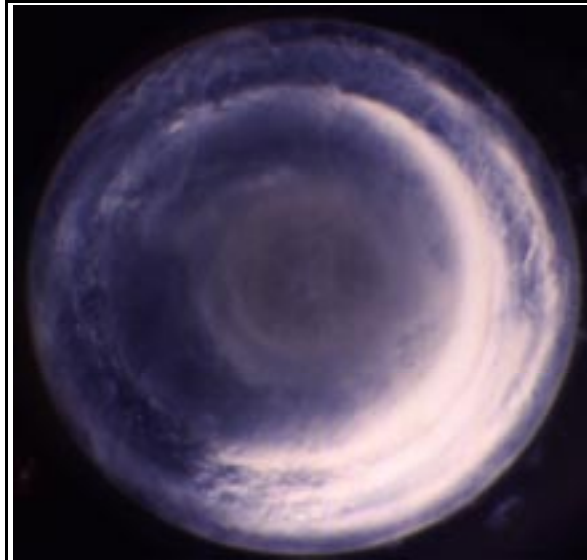


Lenses from rats treated with selenite and with Mn(III)-salophen. The lens on the right shows some posterior subcapsular opacity, but both nuclear regions were transparent.

Figure 2-5 : Mn-Salophen Protected Lenses at 120 hours after Selenite

Long-Term Visual Effects

An additional litter of twelve animals was maintained for nine months after selenite injection to evaluate long-term protective or toxic effects of Mn(III)-salophen/selenite administration. Nuclear transparency was not maintained into adulthood after Mn(III)-salophen/selenite treatment. Animals which had shown protection at 120 hours had a variety of severe nuclear and cortical opacities at the time of killing (Figure 2-6). The lens showed multiple concentric refractile rings as well as dense nuclear opacification. The cortex showed evidence of extensive vacuolarization. In spite of the profound ocular differences between Mn(III)-salophen/selenite treated animals and both positive and negative controls, the entire litter was a uniform weight for their gender. Males weighed 538 ± 16 grams (N = 5) and females weighed 305 ± 5 grams (N=7). Necropsy of positive and negative control animals revealed no gross abnormalities. All Mn(III)-salophen/selenite treated animals had small (< 10%) infarcted tissue areas, either hepatic, renal, or both. No animals had evidence of systemic disease prior to necropsy.



Dark-field microscopic view of a lens from an adult rat 9 months after selenite injection and subsequent high-dose Mn(III)-salophen treatment. The lens is extensively liquified around a dense NC and large numbers of vacuoles have formed.

Figure 2-6 : Long-term Effect of Mn-Salophen/Selenite Treatment

Cross-contamination

To measure protection from cataract formation, Mn(III)-salophen/selenite animals were initially compared with positive control animals from their own litter. The extent of cataract formation in positive controls whose littermates had been treated with Mn(III)-salophen in DMSO did not correlate with lenses from other positive control animals. In litters with only positive and negative control animals, all positive controls developed bilateral stage 3 PSOs after one day and full nuclear cataracts within five days. In litters with Mn(III)-salophen present, although all positive control animals had visual disturbances, in up to 50% of positive control animals they were incomplete, failing to develop complete PSOs or NCs. This phenomenon is probably due to contamination of the positive control animals by fluid leaking from injection sites of their Mn(III)-salophen-treated littermates. After this discovery, comparisons to measure protection were made with positive controls from litters not treated with Mn(III)-salophen.

Discussion

Visual Effects

Given the published reports of the generation of superoxide within a selenite and glutathione reaction system, it was plausible that a superoxide radical scavenger might be of some benefit *in vivo* against selenite-mediated damage. We found Mn(III)-salophen did protect from cataractogenesis in the short-term. The early effect of diminished PSO formation was reproducible and of interest but was not chosen for exhaustive study because of the lack of quantitative information available about PSO formation and resolution in the selenite cataract model. Individual separation of affected fibers from unaffected ones would be very difficult in a wet lens, and therefore quantitative changes would have been difficult to measure. Once the dosage for Mn(III)-salophen was increased to the level which affected NC significantly, it was more practical to focus on the nuclear phenomenon.

The effect of Mn(III)-salophen on NC was remarkable, although the retention of PSO at 120 hours is suggestive of an arrest of cataract formation rather than a reversal of damage. The failure of Mn(III)-salophen to provide long-term protection against cataracts also supports the hypothesis that the cataractogenic process has been temporarily suspended.

The morphology of the lenses from animals kept long-term after Mn(III)-salophen/selenite administration was very different from that of positive controls kept for a similar period. Positive control lenses retained a dense nuclear cataract indefinitely, but the remainder of the lens grew normally, leaving a clear cortex. In Mn(III)-salophen/selenite treated animals, the lens cortex was severely perturbed, indicating a continuing derangement of lens metabolism. It is possible that the side effects of Mn(III)-salophen treatment are more than the lens can withstand after the selenite insult.

The choice of DMSO as a solvent was based on its ability to dissolve Mn(III)-salophen at a higher concentration than was possible in ethanol. The bioavailability of DMSO in the lens of an adult rat was low,⁴⁰ but data were not available for neonates. DMSO was present in much higher amounts in the vitreous humor and blood than in the lens of adult rats.⁴⁰ It was reasonable to believe that the neonatal vascular bed which allows for delivery of selenite also facilitated DMSO-based Mn(III)-salophen transport. If this transport method is critical it could explain the young developmental size of under 25 grams, necessary for Mn(III)-salophen efficacy.

Toxicity

Once we had established an effective dose for Mn(III)-salophen we discontinued further pharmacological trials. For that reason we have not established an LD₅₀. The toxicity due to ethanol administration was not unreasonable, given that animals were immature and less able to detoxify alcohol. DMSO-based preparations of Mn(III)-salophen caused high mortality (~50%) if not given within 1-2 days of synthesis. This observation was

explained by the formation of toxic sulfones by DMSO and oxygen, as it was not seen with DMSO-based Mn(III)-salophen that had been sparged with argon.

Some animals died due to complications of intraperitoneal injection, such as inadvertent laceration of internal organs or major blood vessels. We identified such animals by necropsy and did not consider those deaths as due to toxicity associated with Mn(III)-salophen. Most unexpected deaths were due to mechanical trauma. These deaths were minimized with time and practice of the procedure. If Mn(III)-salophen was injected into an animal which was significantly underweight for gestational age (nominal values 18-25g at 10-12 days old) such mortality was significantly increased. This problem was resolved by eliminating litters with large disparity in animal weights.

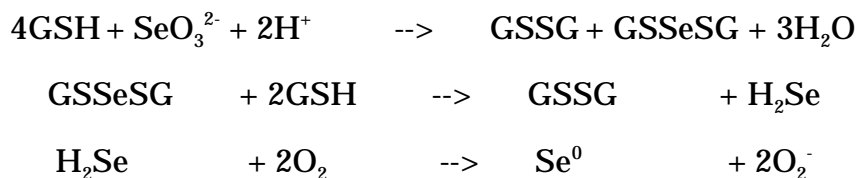
3. *IN VITRO* EFFECT OF Mn(III)-SALOPHEN ON THE REACTION BETWEEN GLUTATHIONE AND SODIUM SELENITE

Introduction

Sodium selenite has been reported to be an antioxidant as well as a chemotherapeutic agent toxic to neoplastic cells.⁹⁵ Selenium is required nutritionally to synthesize the amino acid selenocysteine, which is essential to the antioxidant enzyme glutathione peroxidase. Animals deficient in selenium are not able to cope well with oxidative insult, so selenium supplementation can serve as an indirect antioxidant. In higher concentrations, selenite can be toxic.¹⁰³

Selenite causes an oxidative stress through its reaction with the tripeptide glutathione. In the presence of selenite, reduced glutathione (GSH) rapidly oxidizes to GSSG. During this oxidation, the intermediate metabolite selenodiglutathione (GSSeSG) is formed. GSSeSG is further reduced to selenide, which generates the oxidative stress by reducing molecular oxygen to superoxide radical (Equation 3-1). These glutathione-containing species can be separated by reverse-phase high performance liquid chromatography (HPLC).¹¹

Equation 3-1 : Oxidation of GSH by Selenite



Sodium selenite is used in an oxidative cataract model. When administered to neonatal rats in a single SQ 30 $\mu\text{mol/kg}$ dose, bilateral nuclear cataracts are generated within five days. This cataract formation is preceded by a decrease of lenticular glutathione, presumably through reaction with selenite. The *in vitro* reaction of selenite with glutathione is used as the basis to study the *in vivo* oxidative stress.

The superoxide scavenger Mn(III)-salophen prevents formation of the nuclear cataracts in the selenite cataract model (Chapter 2). By examining the effect of Mn(III)-salophen, as well as that of the antioxidant enzymes superoxide dismutase and catalase, upon the *in vitro* reaction, we sought to determine a mechanism by which Mn(III)-salophen may protect *in vivo*. Because Mn(III)-salophen is a known radical scavenger, we explored the possibility of free radical detection in this system by electron paramagnetic resonance (EPR). We also modeled the molecular structure of Mn(III)-salophen to understand better its potential *in vivo* chemistry responsible for cellular protection against oxidative stress.

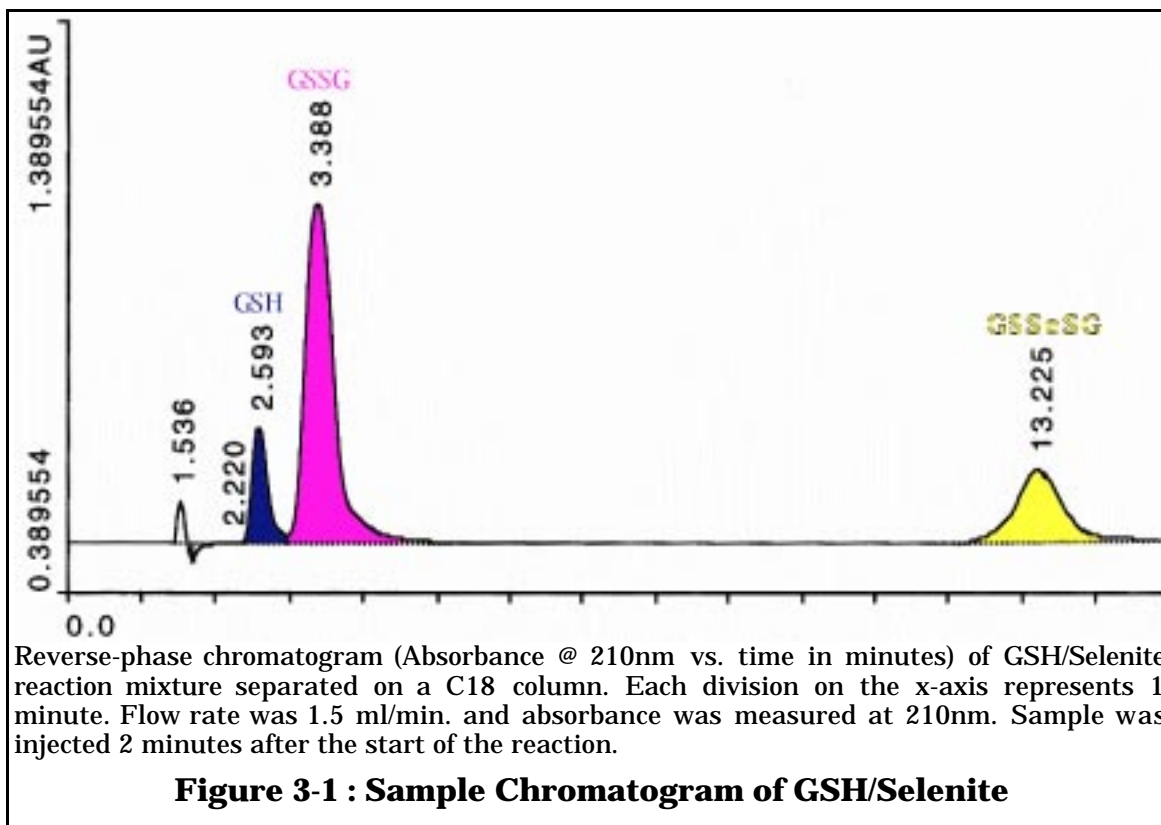
Materials and Methods

Preparation of Mn(III)-salophen

See Chapter 2 : Administration of Mn(III)-salophen And Its Preservation Of Lens Transparency In Rats.

HPLC Separation of Glutathione Oxidation Products by Selenite

The *in vitro* reaction of GSH with sodium selenite was typically carried out at a 10:1 concentration ratio (1 mM GSH / 100 μ M selenite or 2 mM GSH / 200 μ M selenite) in 50 mM sodium phosphate buffer, pH 7.4. The reaction was initiated by the addition of GSH. The oxidative products of the reaction of GSH with sodium selenite were measured by HPLC in a mobile phase of 4% ammonium phosphate over a reverse phase C18 column with detection at 210nm.¹¹ The two instruments used over the course of the study were a Waters 501 gradient pump system with Waters 484 UV/Vis Detector and a U6K Injector, and a Rainin Dynamax SD-200 Pump controlled by Rainin Dynamax HPLC software running on a Macintosh IIsi. Precision injection volumes were ensured by using Hamilton gas-tight syringes (25, 100, or 250 μ l) and either overfilling with 2.5 X nominal loop volume of 20-100 μ l or by underfilling a 2 ml loop. Distinct peaks were measured for each of the species GSH, GSSG, and GSSeSG. (Figure 3-1) No reaction occurred in the absence of either GSH or selenite.



Separate peaks for DMPO and DMSO were recorded when either was present in the reaction mixture. The absorption from known quantities of GSH and GSSG were measured and calibration curves determined. The retention times varied by less than 10%. Concentrations were determined \pm 5 mM, based on total integrated area for each peak. The reaction was carried out in the presence of MnSOD, Mn(III)-salophen, Mn(III)-acetate, salophen, catalase, and DMPO, individually or in combinations.

Electron Paramagnetic Resonance (EPR) Studies

The presence of radical species in the GSH/Selenite reaction mixture was examined using EPR. The instrument was calibrated using a standard reaction mixture of 8.3 mM FeSO₄ and 0.3 mM H₂O₂, in the presence of 0.83 mM EDTA and 100 mM DMPO. The GSH / selenite reaction mixture was prepared similarly to that described for HPLC studies above. The EPR spectrum was measured on an IBM Electron Paramagnetic Resonance Instrument located in the laboratory of Dr. H. Misra, Dept. of Biomedical Sciences and Pathobiology, VA-MD Regional College of Veterinary Medicine. Instrument settings were: receiver frequency 100 kHz, field 1 G, gain 4.0×10^5 , time constant 0.640 s, phase 270 degrees. Samples were individually loaded into capillary tubes (~70-80 μ l/tube) and placed into the detection chamber.

Molecular Modeling of Mn(III)-salophen

The structure of Mn(III)-salophen was modeled using QUANTA version 4.0 on a Silicon Graphics Personal IRIS workstation. Minimization of energy state was carried out using alternating steepest descents and adopted-basis-Newton-Raphson techniques with a CHARMM computation engine. Molecular dynamics studies were simulated for 30ps at a temperature of 300 K.

Results

Oxidation of GSH by sodium selenite in vitro

Selenite catalyzes the autooxidation of GSH to GSSG *in vitro*.⁹⁵ At 10 : 1 ratio of GSH to selenite, the GSH was rapidly oxidized to GSSG, with formation of the intermediate species GSSeSG. (Table 3-1 and Figure 3-2). By one minute after the start of the reaction, the intermediate species reached a maximum concentration of 180 μ M. The reaction had essentially reached completion at four minutes, when it contained 620 μ M GSH, 640 μ M GSSG, and 9 μ M GSSeSG. A four minute maximum lifetime for GSSeSG under these reaction conditions was consistent with literature reports for this reaction.⁹⁵

Table 3-1 : Reduction of Selenite by Glutathione

HPLC measurement of glutathione metabolites. Initial Concentrations: GSH 2 mM; Selenite 200 μ M; in phosphate buffer pH 7.4 Concentrations were calculated $\pm 5 \mu$ M, Times were measured ± 0.1 min.

time (min.)	GSH (mM)	GSSG (mM)	GSSeSG (mM)
0	2.000	0.000	0.000
0.5	0.942	0.162	0.096
1	0.683	0.315	0.180
1.5	0.618	0.469	0.117
2	0.639	0.553	0.057
4	0.621	0.641	0.009

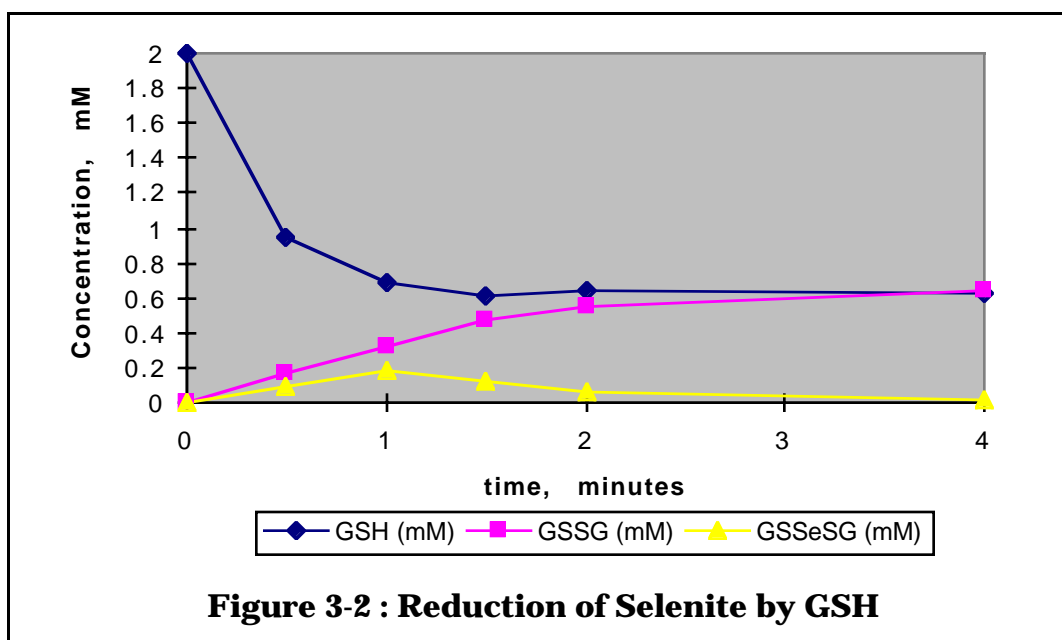


Figure 3-2 : Reduction of Selenite by GSH

Effect of Mn(III)-salophen and Mn(III)-acetate.

Experiments were carried out to measure the effect of Mn(III)-salophen on this reaction. A DMSO peak appeared when used as a vehicle for Mn(II)-salophen, but did not interfere with other peaks. Mn(III)-salophen was added to the reaction mixture before the initiation of selenite reduction by GSH.

Adding 200 μ M Mn(III)-salophen increased the lifetime of the intermediate GSSeSG and resulted in a final composition of 22 μ M GSH, 460 μ M GSSG, and 49 μ M GSSeSG at 20 minutes. The addition of 200 μ M Mn(III)-salophen to the reaction mixture resulted in a preservation of selenodiglutathione as well as a lower final amount of reduced glutathione. At twenty minutes after the start of the reaction, selenodiglutathione concentration was 67% (49 μ M) of its maximum value, compared to 5% after only four minutes in the absence of Mn(III)-salophen (Table 3-2 and Figure 3-

3). The concentration of reduced glutathione fell to 2% (22 μ M) of its starting value in the presence of Mn(III)-salophen, compared to 31% without Mn(III)-salophen.

Table 3-2 : Effect of 200 μ M Mn-salophen upon GSH/Selenite reaction

HPLC measurement of glutathione metabolites. Initial Concentrations: GSH 1 mM; Selenite 100 μ M; Mn(III)-salophen 200 μ M; in phosphate buffer pH 7.4; Concentrations were calculated ± 5 μ M, Times were measured ± 0.1 min.

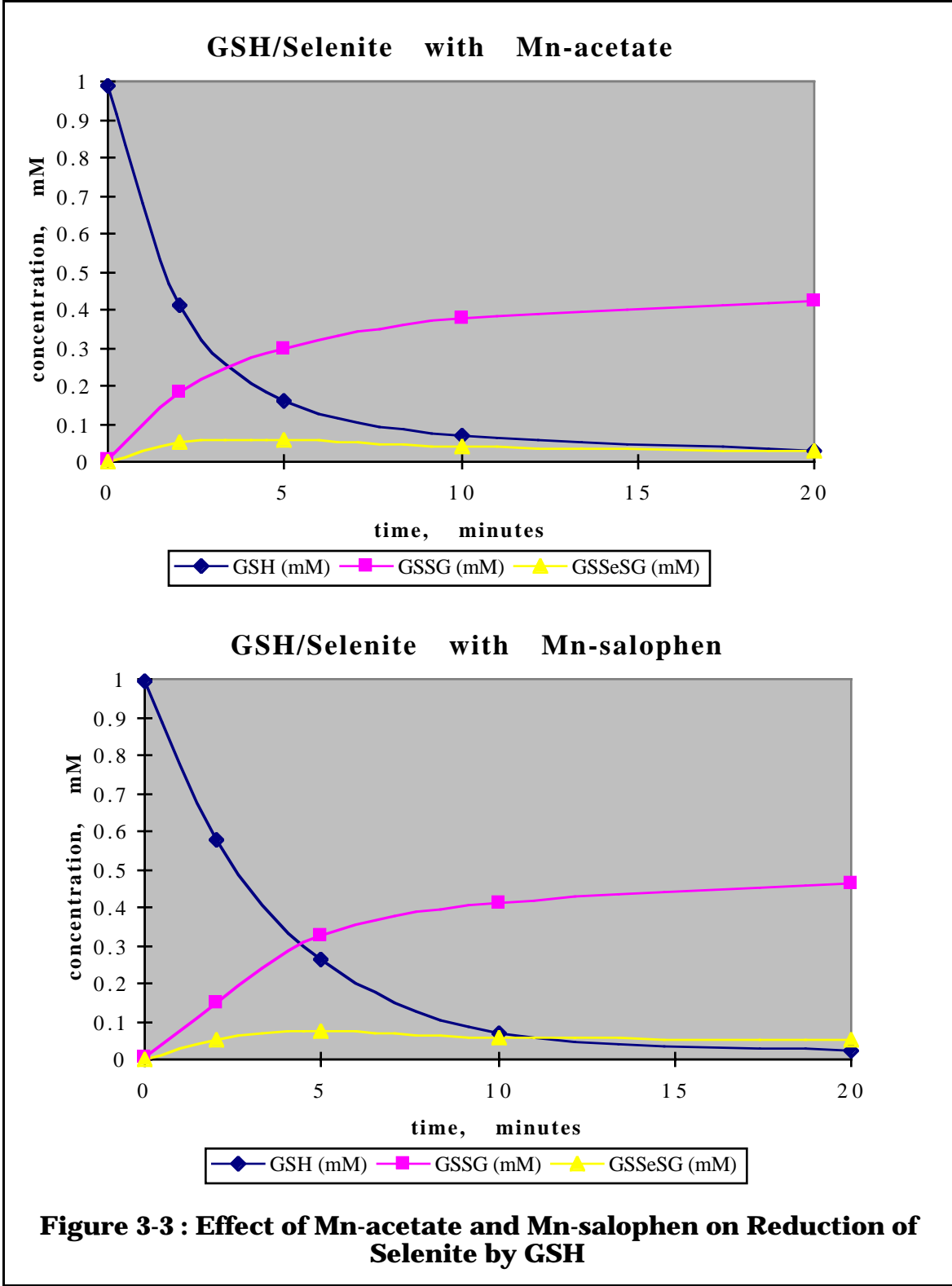
<i>time (min.)</i>	<i>GSH (mM)</i>	<i>GSSG (mM)</i>	<i>GSSeSG (mM)</i>
0	0.996	0.004	0.000
2	0.578	0.149	0.054
5	0.261	0.324	0.073
10	0.067	0.412	0.060
20	0.022	0.461	0.049

The selenodiglutathione level decreased to very low quantities within five minutes when Mn(III)-salophen was not present, but remained near its maximum when Mn(III)-salophen was added. Using Mn(III)-acetate instead of Mn(III)-salophen produced a similar result, though the GSSeSG levels decreased faster (Table 3-3 and Figure 3-3). Adding the ligand salophen alone had no effect on the reaction.

Table 3-3 : Reduction of Selenite by GSH (with 200 μ M Mn-acetate)

HPLC measurement of glutathione metabolites. Initial Concentrations: GSH 1 mM; Selenite 100 μ M; Mn(III)-acetate 200 μ M; in phosphate buffer pH 7.4; Concentrations were calculated ± 5 μ M, Times were measured ± 0.1 min.

<i>time (min.)</i>	<i>GSH (mM)</i>	<i>GSSG (mM)</i>	<i>GSSeSG (mM)</i>
0	0.991	0.004	0.000
2	0.413	0.183	0.050
5	0.162	0.295	0.056
10	0.069	0.376	0.041
20	0.027	0.423	0.029

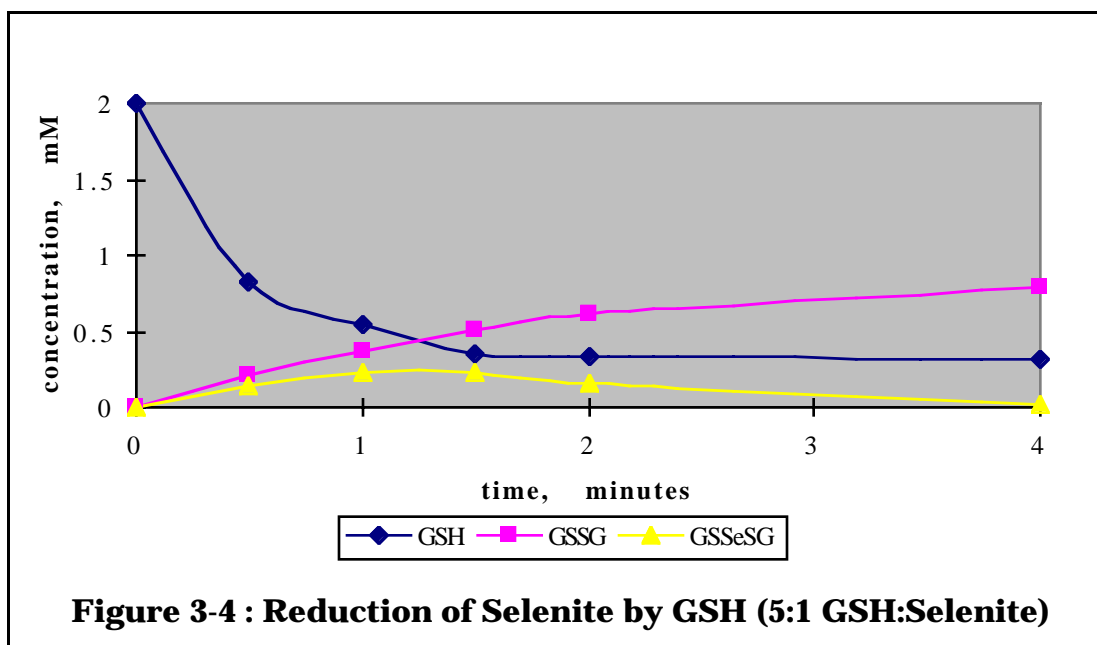


The effect of limiting GSH was examined by varying the relative initial concentration of GSH and selenite. Doubling the amount of selenite (net ratio 5:1 GSH:Selenite) produced a higher GSSeSG level of 225 μM and a final GSH level of 324 μM . The final GSSeSG concentration dropped to 26 μM , indicating that the reaction progressed (Table 3-4).

Table 3-4 : Reduction of Selenite by GSH (5:1 GSH:Selenite)

Reaction of 2 mM GSH with 400 μM Selenite in phosphate buffer, pH = 7.4 . Metabolites levels were presented in mM \pm 5 μM . Reaction times were \pm 0.1 min.

<i>time (min.)</i>	<i>GSH</i>	<i>GSSG</i>	<i>GSSeSG</i>
0.0	2.000	0.000	0.000
0.5	0.828	0.204	0.132
1.0	0.549	0.363	0.225
1.5	0.354	0.509	0.225
2.0	0.337	0.609	0.165
4.0	0.324	0.787	0.026



Lowering the GSH concentration from 2 mM to 1 mM with a selenite concentration of 400 μM resulted in an incomplete reduction of selenite. GSH was completely depleted to less than 10 μM by 4 minutes after the start of the reaction. GSSeSG was at a maximum level of 0.23 mM and did not break down. A peak representing either selenite or an intermediate that formed before GSSeSG remained. This peak correlated to a suspected glutathione-selenite adduct seen previously (Ware and Hess, unpublished data).

Table 3-5 : Reduction of Selenite by GSH (5:2 GSH:Selenite)

HPLC measurement of glutathione metabolites. Initial Concentrations: GSH 1 mM; Selenite 400 μ M; in phosphate buffer pH 7.4; Concentrations were calculated ± 5 μ M, Times were measured ± 0.1 min.

<i>time, min.</i>	<i>GSH, mM</i>	<i>GSSG, mM</i>	<i>GSSeSG, mM</i>
0	2	0	0
0.5	0.786	0.149	0.094
1	0.522	0.239	0.164
2	0.118	0.260	0.213
3	0.047	0.336	0.228
4	0.038	0.355	0.218

Adding the DMSO vehicle alone to the reaction mixture did not affect the lifetime of selenodiglutathione. (Table 3-6)

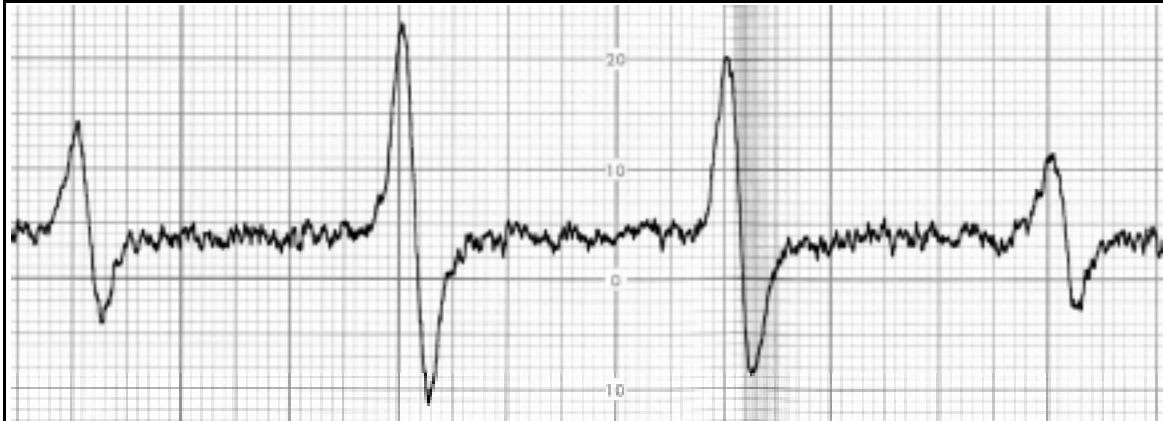
Table 3-6 : Reduction of Selenite by GSH (with DMSO)

HPLC measurement of glutathione metabolites. Initial Concentrations: GSH 1 mM; Selenite 100 μ M; DMSO 5 μ l 100%; in phosphate buffer pH 7.4; Concentrations were calculated ± 5 μ M, Times were measured ± 0.1 min.

<i>time, min.</i>	<i>GSH, mM</i>	<i>GSSG, mM</i>	<i>GSSeSG, mM</i>
0	0.982	0.005	0.000
2	0.299	0.096	0.079
5	0.294	0.164	0.012
10	0.247	0.179	0.009
20	0.240	0.184	0.006

Electron Paramagnetic Resonance (EPR) Studies

Identification of radical species present in the reaction which could be affected by the presence of Mn(III)-salophen was attempted by EPR. Reaction mixtures were as described above with the addition of 50 mM DMPO. The instrument was calibrated with solutions generating hydroxyl radical (Figure 3-5) and TEMPO. Reaction ratios of 10:1 and 5:1 GSH:Selenite were used. Samples taken at less than one minute, five minutes, and ten minutes after addition of GSH were scanned. No signal corresponding to either a thiyl or superoxide radical was found during the reaction of GSH with selenite. Addition of 1mM EDTA did not affect the signal.

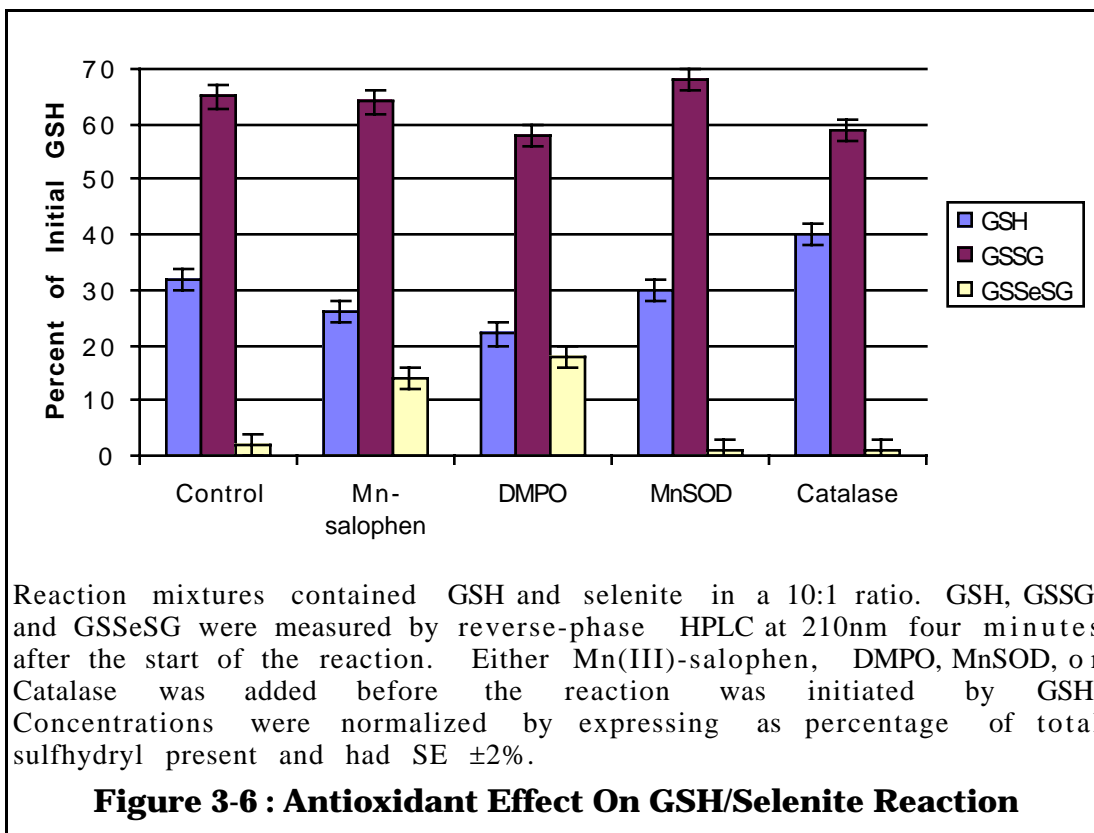


Radical signal from HO•. Signal was measured by EPR as described in materials and methods, above.

Figure 3-5 : EPR Calibration Signal from Hydroxyl Radical

Effect of DMPO, MnSOD, and Catalase on GSH Oxidation by Selenite

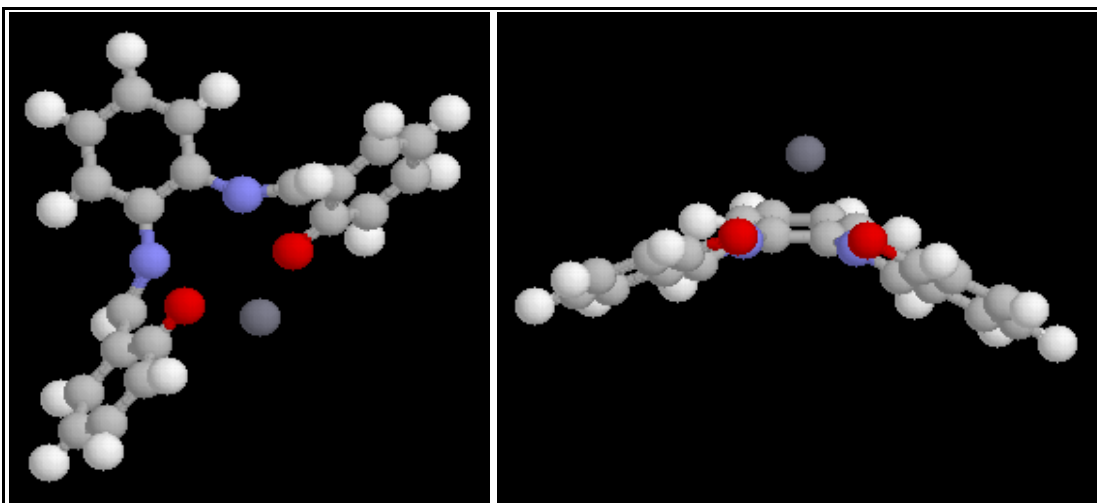
In the presence of the spin-trap DMPO, the reaction behaved very similarly to when Mn(III)-salophen was present. The level of seleno-diglutathione was preserved beyond its nominal lifetime and the reduced glutathione level fell further than in the absence of DMPO. In contrast, the enzymes superoxide dismutase and catalase had no effect on the lifetime of GSSeSG. A comparison at 4 minutes after the start of the reaction shows the effect of various species on the lifetime of GSSeSG (Figure 3-6).



Modeling of Mn(III)-salophen

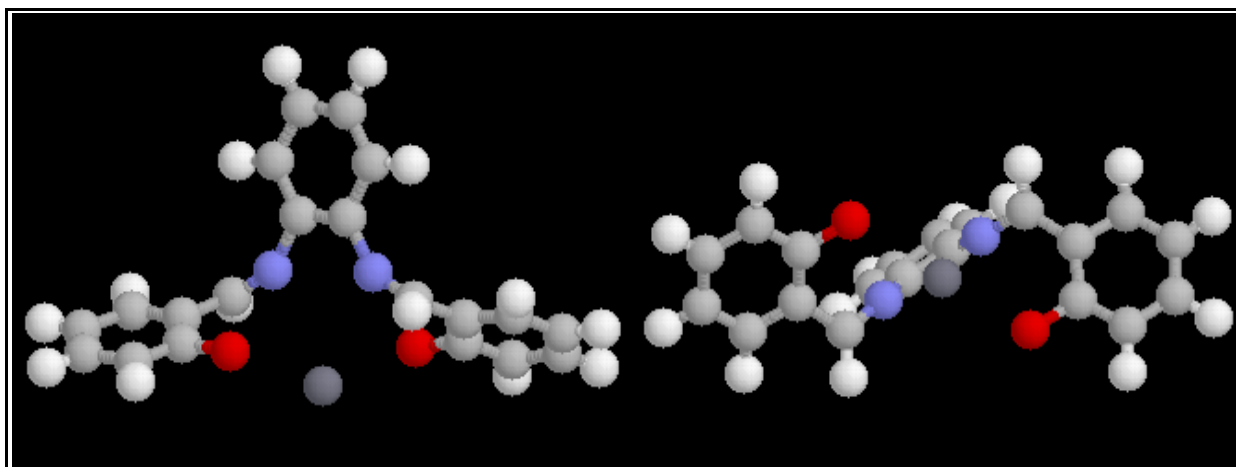
In an attempt to better understand the structure of Mn(III)-salophen and thereby predict likely behavior in different solvents and under cellular conditions, a molecular structure was modeled. Mn(III)-salophen has been shown to have a maximal superoxide scavenging activity when its synthetic components Mn(III)-acetate and salophen are mixed in a 1:1 ratio.⁷² The salophen ligand has several residues which could interact with and stabilize the manganese ion: two imine nitrogens, each with a free pair of electrons; and two hydroxyl groups, which could hold a partial negative charge.

Two stable structures were generated during the minimization experiments. Neither was able to fit the Mn³⁺ ion between salophen's free phenyl rings due to the size of the metal. One configuration appeared to chelate from one side only (Figure 3-7), while the other chelated from both sides. (Figure 3-8)



One-sided potential structure of Mn(III)-salophen. Structure was generated using Quanta on a Silicon Graphic Personal Iris System. The color system is as follows: manganese ion dark gray, carbons light gray, hydrogens white, nitrogens blue, and oxygens red.

Figure 3-7 : One-sided Structure of Mn(III)-salophen



Two-sided potential structure of Mn(III)-salophen. Structure was generated using Quanta on a Silicon Graphic Personal Iris System. The color system is as follows: manganese ion dark gray, carbons light gray, hydrogens white, nitrogens blue, and oxygens red.

Figure 3-8 : Two-sided Structure of Mn(III)-salophen

Molecular dynamics were carried out on both potential structures. The two-sided structure appears to have less accessibility to solvent, and was predicted to have a higher stability during the simulation. After molecular dynamics simulation at 300 K, the two-sided structure “lost” Mn, as the ion left the chelation range of the salophen. During the simulation it appeared that both oxygens were involved in bonding with Mn, but neither nitrogen. In contrast, the one-sided structure maintained at least three of its four available

residues actively bonding to Mn, and remained stable throughout the simulation.

Discussion

The end product of selenite reduction by glutathione is selenide, which can inactivate other enzymes by a oxidative mechanism involving superoxide.¹² Given the reportedly higher toxicity of the selenodiglutathione intermediate, the late generation of superoxide in this mechanism has been reported to cause oxidative stress related to selenite injection.

If this postulated mechanism were correct, Mn(III)-salophen could scavenge superoxide from the end of the pathway, but we would not expect to see an effect of Mn(III)-salophen upon the major species (GSH, GSSG, GSSeSG). The preservation of GSSeSG by Mn(III)-salophen is revealing. Previous work in our laboratory indicated that Cu/Zn SOD, the principal eukaryotic form, did not affect the lifetime of GSSeSG, (Hess and Smith, unpublished data) which was consistent with the published mechanism. We examined the effect of MnSOD upon the reaction as well, and also found no preservation of GSSeSG. Clearly, the mechanism of Mn(III)-salophen interference was different from that of a SOD.

The other significant observation was the lower level of GSH present at the end of the reaction in the presence of Mn(III)-salophen with the preserved GSSeSG (Figure 3-3). If Equation 3-1 were correct and GSH were oxidized in the breakdown of GSSeSG, then stopping that breakdown of GSSeSG should result in higher levels of GSH at the end of the reaction, with a correspondingly lower GSSG level.

By adjusting the relative concentrations of GSH and selenite to 5:1, it became clear that the breakdown of GSSeSG continues after the level of GSH has reached its minimum (

Figure 3-4). GSSG continues to be produced in this process, which can cause an apparent shift in oxidized/reduced ratio of glutathione; however, net oxidation of GSH is not occurring. In a 5:2 ratio, glutathione is limiting, and GSSeSG is preserved. If GSH is necessary for the breakdown of GSSeSG, but is not consumed, then it must exist in a steady state.

In vivo, the breakdown of selenodiglutathione is catalyzed by the enzyme thioredoxin reductase, which consumes reducing equivalents in the form of NADPH. In doing so, it releases GSH.¹¹ If the *in vitro* system, lacking NADPH, were to have a similar mechanism, there must be another reducing agent present. We propose that another reductive species generated during the reduction of selenite to selenodiglutathione acts similarly to NADPH in the thioredoxin reductase system. Such a release of GSH during the breakdown of GSSeSG would then correlate with present observations.

The identity of this reducing agent is unknown. Given the one-electron scavenging activity of Mn(III)-salophen, it was possible that a radical species

was responsible. That DMPO preserves GSSeSG in a similar response to Mn(III)-salophen, seemed to indicate that the two act with a similar mechanism. Unfortunately, no radical signal was detected by EPR in the GSH/Selenite reaction although the instrument effectively measured a hydroxyl radical signal (Figure 3-5). The presence of excess GSH in a reaction mixture can hydrolyze DMPO radical adducts in the presence of trace metals; however, adding the metal chelators EDTA or DTPA had no effect upon the signal.

The prolonging of GSSeSG's lifetime revealed that DMPO perturbed the reaction conditions. Moreover, it seemed unlikely that a simple abstraction of radicals was responsible for the changes, as no EPR signal was present. The exact nature of the reducing species that is consistent with these results is unknown. However, it could be a ROS. DMSO will scavenge hydroxyl radicals,⁹⁷ but did not affect GSSeSG lifetime in our test system, so hydroxyl radical formation seems unlikely. If the responsible species were superoxide radical, we would expect SOD to have a similar effect as Mn(III)-salophen, stabilizing GSSeSG.

The mechanism for removal of oxygen from selenite has not been established. In order for another reducing species to be generated, the oxygens cannot be reduced completely to water. To resolve these inconsistencies, an alternate reaction for the generation of selenodiglutathione is proposed:



Mn(III)-salophen is known to inactivate both superoxide and hydrogen peroxide, and by intercepting the hydrogen peroxide generated in the earliest part of the reaction, the reaction would halt at GSSeSG. The hydrogen peroxide produced could explain a report by Spallholz that catalase inhibits superoxide production in the GSH-dependent reduction of selenite.¹⁰⁵ Hydrogen peroxide could subsequently be consumed in the reduction of GSSeSG as follows:

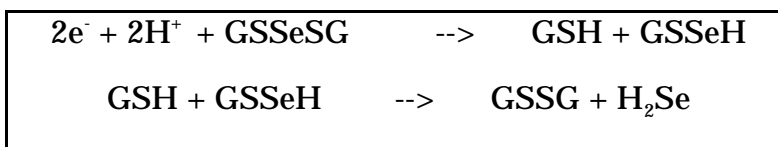
Equation 3-3 : Breakdown of GSSeSG—Proposal A



Equation 3-3 requires a steady state level of GSH for the breakdown of GSSeSG. This cycling of GSH is consistent with our data indicating that net oxidation of glutathione is zero during the breakdown of GSSeSG. (

Figure 3-4) A second possibility involves the direct use of the reducing equivalents generated in the GSSeSG-producing reaction. These electrons would substitute for hydrogen peroxide in Equation 3-3 as follows:

Equation 3-4 : Breakdown of GSSeSG—Proposal B



In either case (Equation 3-3 or Equation 3-4) the oxidation state of selenium would change from 2^+ to 2^- , resulting in the formation of selenide. A removal of the reducing agent would prevent selenodiglutathione from proceeding to selenide, thereby forestalling the superoxide radical generation that would ensue. Other mechanisms have been proposed to explain inhibition of superoxide generation in this system. For example, metal complexing with selenides is hypothesized to explain the effect of copper and zinc inhibition of superoxide generation by selenite.³⁵ However, such a complexation with an intermediate later in the reaction scheme is unlikely to apply to Mn(III)-salophen, as it would not explain the preservation of selenodiglutathione.

We conclude that Mn(III)-salophen acts in the early reduction of selenite to selenodiglutathione and scavenges an electron carrier which is necessary for rapid metabolism of GSSeSG. This mechanism disables the characteristic oxidative burst in this system and thereby forestalls severe biological damage.

Modeling of Mn(III)-salophen

Modeling transition metal complexes is challenging because of the numerous possible coordinate geometries and ionization states. This salophen complex is particularly difficult because the putative ligands are not simple and are physically constrained.

The low solubility of Mn(III)-salophen in aqueous solution suggests that the polar groups on or near salophen's phenyl rings are occupied through bonding to the metal ion. The higher solubility in DMSO is expected in light of salophen's slightly polar, hydrophobic structure.

The stability of the one-sided form of Mn(III)-salophen would allow stacking of alternating salophen and manganese while maintaining a 1:1 ratio.

4. EFFECT OF *IN VIVO* SELENITE AND MN(III)-SALOPHEN ADMINISTRATION ON LENS ION HOMEOSTASIS AND LENS CRYSTALLIN PROTEOLYSIS

Introduction

Cataracts occur when disruption of the lens matrix causes the formation of light-scattering bodies. They can be caused by a number of factors that include post-translational proteolysis and aggregation of crystallins into high-molecular weight aggregates. Other possible causes include the loss of water and sodium homeostasis, genetic disease causing incorrect crystallin formation, or systemic metabolic disease such as diabetes mellitus.⁶⁸ Many post-translational modifications occur during normal aging and do not necessarily result in cataract formation. In order to identify factors that may be critical to cataract formation, it is reasonable to compare changes seen in cataractous lenses from clear lenses of similar age.

Injection of 30 $\mu\text{mol/kg}$ sodium selenite into ten- to fourteen-day-old rats causes bilateral nuclear cataracts within 5 days.¹⁹ In this cataract model, examination by two-dimensional electrophoresis of the lens crystallins from animals with cataract reveals extensive proteolysis of α - and β -crystallins which does not occur in untreated animals.⁹¹ Additionally, lens calcium homeostasis is lost.²⁰ The pattern of proteolysis seen in selenite-treated rats was replicated when purified lens proteins were treated with the calcium-activated protease *m*-calpain.^{34, 65}

The rat lens has a calcium content much lower than that of the aqueous or vitreous humor.⁸⁵ Within 48 hours of injection of selenite, the lens calcium levels increase, reaching a maximum five days later, when a dense nuclear cataract has formed. The exact manner by which selenite causes the increased calcium is unclear, although lipid peroxidation and damage to the Ca^{2+} -ATPase may contribute to the accumulation of calcium in the lens.^{5, 37} Regardless of mechanism, the elevated calcium activates the calcium-dependent protease *m*-calpain, which catalyzes the proteolysis of α - and β -crystallins. Detailed analysis of lenticular proteins in the selenite model has demonstrated proteolytic patterns consistent with *m*-calpain mediated proteolysis of α - and β -crystallins^{34, 65}. Adding a calpain inhibitor to lens culture prevents selenite-mediated cataractogenesis *in vitro*.³² From these observations, it is currently hypothesized that the loss of calcium homeostasis is a critical result of selenite-mediated oxidative stress.

In lenses from animals treated with 300 $\mu\text{mol/kg}$ of the superoxide scavenger Mn(III)-salophen, the nucleus remains transparent at 120 hours after selenite injection. (Chapter 2) To examine the mechanism by which Mn(III)-salophen protects against cataract formation, levels of protein were quantified, levels of Na^+ , K^+ , and Ca^{++} were measured in the lens and the lens proteins were examined by electrophoresis.

Materials and Methods

Animal Care and Lens Removal

See Chapter 2: Administration of Mn(III)-salophen And Its Preservation Of Lens Transparency In Rats.

Analysis of Lens Proteins

Protein content was analyzed for three groups: whole lens, cortex, and nucleus. To separate nuclear and cortical fractions the lenses were blotted, placed on a clean microscope slide, and punctured along the transverse axis. After cutting a hemispherical incision along the equator, the cortical layers were peeled back from the nucleus and the nuclear region was lifted from the center of the lens. The nucleus was stored in a microcentrifuge tube and the cortex was scraped from the slide into a separate tube. All lens tissue intended for protein analysis was frozen in liquid nitrogen immediately after removal and stored at -20 C. Lens proteins were separated into buffer-soluble, urea-soluble and urea-insoluble fractions. Whole lenses were homogenized in microcentrifuge tubes with a tight-fitting glass pestle in 250 μ l/lens of phosphate buffer (Buffer H) consisting of 1% sodium azide and 5 mM EDTA in 100 mM sodium phosphate at pH 7.2. After centrifugation at 6300 x *g* for 5 minutes, the buffer-soluble supernatant was removed and frozen. The pellet was resuspended in 100 μ l/lens of urea buffer (Buffer H containing 9.5 M urea). After a second, similar centrifugation, the urea-soluble supernatant was removed and frozen. The second pellet was retained as the urea-insoluble fraction. Protein concentrations were determined using the Bradford Coomassie Blue R-250 dye-binding assay,¹⁶ using bovine serum albumin (BSA) as a protein standard.

Separation and Identification of Lens Crystallins

Lens fractions were separated using one- and two-dimensional SDS-PAGE, according to procedures of Lammelli, as modified in the Current Protocols in Molecular Biology.⁴⁷ Forty micrograms of protein were used for each 2-D gel. Isoelectric focusing for the first dimension was carried out according to the instructions in the Hoefer tube gel adapter kit.⁶² The first dimension separation was by isoelectric focusing from pH 3 to 10 in a 1.5 mm ID tube gel. The focused tube gel was loaded on a denaturing (SDS) 12% polyacrylamide slab gel and separated by mass. Gels were fixed and stained according to the Rapid Coomassie Staining/Destaining protocol and were scanned wet using a transparency adapter at 400 dpi on a UMAX Vista S-8 flatbed scanner. Images were processed by NIH Image, version 1.58 and Adobe Photoshop, version 3.0.5. Individual proteins on 2-D gels were tentatively identified according to published reports of sequence and gel data by David and Smith.³⁴

Glutathione content of lenses

Whole lens homogenates were prepared with 10% trichloroacetic acid (TCA) to precipitate protein. The homogenate was centrifuged at 10,000 x *g* for five minutes. Glutathione levels were determined in the supernatant using the coupled DTNB / NADPH / glutathione reductase spectrophotometric assay at 412 nm.¹⁸

Elemental analysis of lenses

Lenses intended for elemental analysis were placed in 0.02 M HEPES buffer with 0.13 M NaCl at pH 7.2. Each lens was washed with 50 μ l of 0.5 mM EGTA, blotted on EGTA-soaked paper, and dried in a desiccator at room temperature to a constant weight. Dried lenses were thoroughly digested with two alternating washes of 200 μ l Optima[®] grade nitric acid (Fisher #A467-250) and 100 μ l of 30% hydrogen peroxide (Fisher #H325-500). For each wash cycle, the samples were placed in a sand bath that was heated to 200°C until the samples had dried. The bath was allowed to cool to room temperature prior to addition of successive digesting reagents. Digested samples were suspended in 3 ml of 10% Optima[®] grade hydrochloric acid (Fisher #A466-250, diluted 1:10 with ddH₂O in calcium-free glassware) then assayed for calcium, sodium, potassium, and sulfur or manganese content by Induced-Coupled Plasma (ICP) spectroscopy at the Soil Testing Laboratory of Virginia Tech. Glassware was considered to be calcium-free after thorough washing followed by rinsing with concentrated nitric acid and ddH₂O.

Results

Effect of Mn-Salophen and Selenite on Animal and Lens Weight

At 72 hours after selenite injection, both the positive control animals and their lenses were approximately 10% smaller than their negative control littermates. (Table 4-1) The lenses showed a proportional decrease in dry weight, indicating no change in hydration state.

At the 120 hour timepoint, the trend in weight differences was still depressed for positive controls and Mn-Salophen/Selenite treated animals, although the positive controls had only a 7.5% weight depression compared to 9.7% at 72 hours. Lens weights did not increase from 72 to 120 hours in the Mn(III)-salophen/selenite group, and only increased slightly in the positive control group. The negative control group and Mn(III)-salophen treatment group lenses grew consistently.

The hydration of the lens remained constant at 72 and 120 hour timepoints for all samples at $69 \pm 2\%$ (w/w). Mn(III)-salophen did not protect against weight loss, either generally in the animal or specifically in the lens.

Table 4-1 : Effect of Selenite and Mn(III)-salophen upon Animal Weight and Lens Weight 72 and 120 hours after Selenite Treatment

Lenses were blotted to remove external water prior to obtaining wet weights and dried in a desiccator at room temperature prior to obtaining dry weights. Values reported represent means \pm SE.

<i>72 hour data</i>	<i>N</i>	<i>Animal Wt (g)</i>	<i>Lens Pair Wet Wt (mg)</i>	<i>Lens Pair Dry Wt (mg)</i>	<i>Pct Water</i>
(-) controls	6	29.1 \pm 0.6	24.2 \pm 0.4	7.8 \pm 0.1	68%
Mn-Salophen	6	28.4 \pm 0.8	24.3 \pm 0.3	7.4 \pm 0.6	70%
Mn-S/Selenite	6	25.8 \pm 0.7	22.9 \pm 0.5	7.0 \pm 0.1	69%
(+) controls	6	26.3 \pm 0.9	22.8 \pm 0.4	7.1 \pm 0.1	69%

<i>120 hour data</i>	<i>N</i>	<i>Animal Wt (g)</i>	<i>Lens Pair Wet Wt (mg)</i>	<i>Lens Pair Dry Wt (mg)</i>	<i>Pct Water</i>
(-) controls	4	34.6 \pm 0.7	26.1 \pm 1.0	8.3 \pm 0.2	68 %
Mn-salophen	4	34.5 \pm 0.5	26.0 \pm 1.0	8.6 \pm 0.3	67 %
Mn-s/Selenite	4	29.3 \pm 1.3	22.1 \pm 0.6	6.8 \pm 0.3	69 %
(+) controls	5	32.0 \pm 2.2	23.5 \pm 0.9	6.9 \pm 0.2	70 %

Lens Protein Quantities and Solubility in Buffer or Urea

When total lenticular protein was measured as the sum of buffer-soluble and urea-soluble protein 120 hours after selenite injection, the lenses of positive controls contained less protein than their negative control littermates. This difference was both an absolute loss of protein and a relative loss, as compared to the wet weight of the lens. A negative control animal had a protein content of nearly 31%, consistent with the water content reported above and very close to the adult nominal level of 33%. The lens from a selenite-treated rat had a protein concentration of below 28%. This relative loss is in addition to the absolute loss of animal and lens weight.

Treatment of animals with both Mn(III)-salophen and selenite partially protected against lenticular protein loss. The total protein recovered from a Mn(III)-salophen/selenite treated lens pair at 120 hours was 8.0 mg, intermediate between the positive and negative control values (Table 4-2).

Table 4-2 : Total Lens Protein and Relative Solubility 120 hours after Selenite Injection

Mean total protein is given for lens pairs. Estimated SE are 10% of mean.

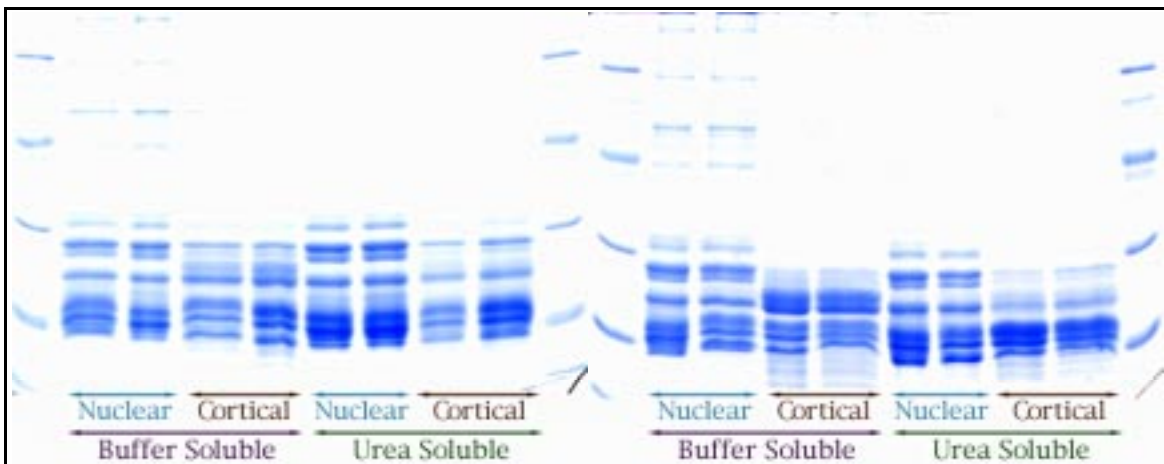
	<i>total protein (mg)</i>	<i>Pct Protein (by weight)</i>	<i>Rel Urea-soluble</i>	<i>Rel Buf-soluble</i>
(-) controls	9.0	30.8 %	7.5 %	92.5 %
Se+Mn-S	8.0	ND	11.1 %	88.9 %
(+) controls	6.5	27.6 %	14.9 %	85.1 %

In addition to the loss of total protein, a selenite-treated lens has twice the amount of buffer-insoluble protein compared to an untreated lens at 120 hours

after selenite treatment. The selenite-dependent increase in urea-soluble protein is less with Mn(III)-salophen treatment. A comparison of the fractionation of the lens and the solubility data is consistent with an intermediate state for Mn(III)-salophen/selenite-treated lenses when compared to positive and negative controls.

Electrophoretic separation of lens proteins

To explore specific changes associated with Mn(III)-salophen protection from cataract formation, protein fractions from protected lenses were compared with similar fractions from positive control lenses by one-dimensional SDS-PAGE. In all permutations of buffer and urea soluble protein from nuclear and cortical regions, the crystallins from protected lenses had similar patterns to those from positive controls from the same litter (Figure 4-1). Because α - and γ -crystallin subunits have very similar molecular weights to each other, and the many β subunits have similar, higher molecular weights, a conclusive comparison was not possible with one-dimensional electrophoresis.



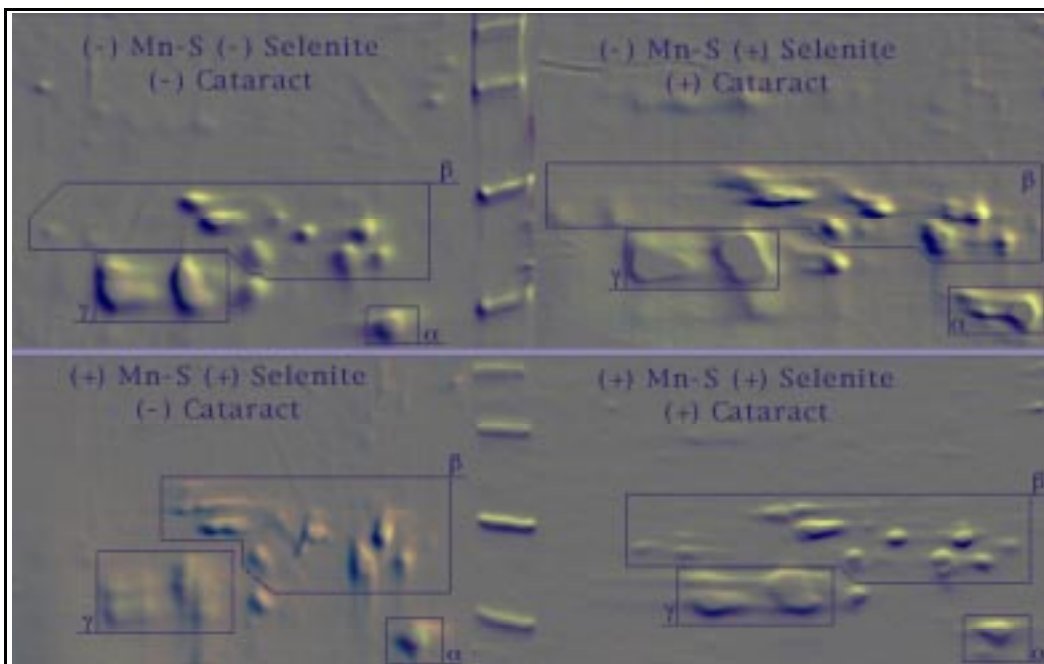
Each group of two lanes represents (+) control and Mn-salophen/selenite treatment groups respectively. Ten micrograms of protein were used for each lane. The 72-hour gel is on the left. Molecular Weight markers are Bio-Rad low range.

Figure 4-1 : One-dimensional SDS-PAGE of Lens Proteins at 72 and 120 hours after selenite injection

To compare protected and unprotected Mn(III)-salophen treated samples with positive and negative controls, two dimensional SDS-PAGE separations were required. To obtain total soluble (both buffer and urea-soluble) proteins in physiological ratios, lens extracts were precipitated with 10% TCA and the pellet was redissolved in urea buffer. Forty micrograms of protein from the lenses of positive control, negative control, protected, and nonprotected groups were examined. The results showed the characteristic pattern of α -, β -, and γ -crystallins in the lenses of negative control animals as

well as the *m*-calpain-proteolyzed pattern of protein from positive control animals. The expected differences in total soluble protein include increased numbers of distinct peptides in the α -crystallin and acidic β -crystallin regions in positive control lenses but similar patterns in the γ -crystallin region (Figure 4-2).

Regardless of protection from visual cataract, treatment with Mn(III)-salophen limited the degree of proteolysis of the α -crystallins. In comparing protected versus nonprotected Mn(III)-salophen/selenite treated lenses, similar patterns of β -crystallins and their fragments were present. The α -crystallins of unprotected Mn(III)-salophen/selenite treated lenses show some degradation not present in protected lenses; however, this degradation is less than that observed in positive controls.

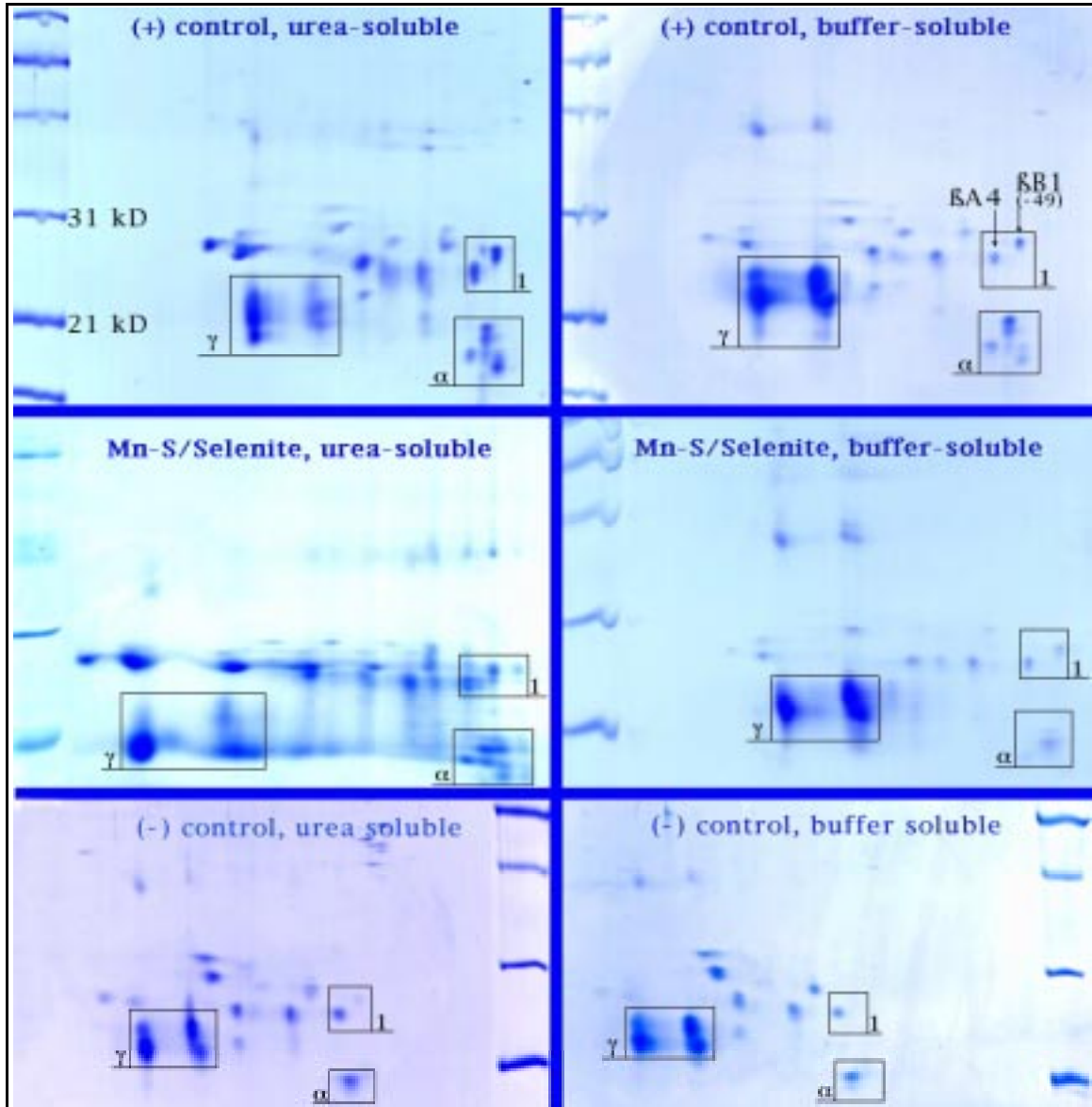


Embossed translations of gel images Proteins were separated by pI in the horizontal dimension (pH 3 to 10, basic on left) and by mass in the vertical dimension (Bio-Rad low-range markers. The top of the β -crystallin box is the 31kD marker). Total (buffer and urea) soluble proteins from negative control lenses (untreated), positive control lenses unprotected lenses (+Se, + Mn(III)-salophen, NC), (+Se, NC), and protected lenses (+Se, + Mn(III)-salophen) {clockwise from top left}

Figure 4-2 : Two-Dimensional Gels of Total Soluble Protein from Rat Lens

To explore differences associated with the nuclear cataract, the nuclear region of positive controls, negative controls, and protected Mn(III)-salophen/selenite treatment groups were separated into buffer and urea soluble protein fractions. When comparing positive control to negative control lenses, we see extensive α -crystallin breakdown, with six distinct spots present

in both buffer and urea-soluble fractions, compared to one major protein in the negative control. Our protected lenses from animals treated with Mn(III)-salophen showed much less proteolysis in the buffer-soluble fraction, with three major spots, but much more in the urea-soluble fraction, with at least nine and possibly eleven distinct species (Figure 4-3).



2-D Gels of nuclear fractions from lenses 120 hours after selenite injection. Proteins are mapped over a pH = 3-10 range (basic end is left on scans above) Except for those boxes labeled a or g, proteins in the 25-35kD range represent β -crystallins. Box 1 contains a representative sample of the extent of proteolysis present under various conditions.

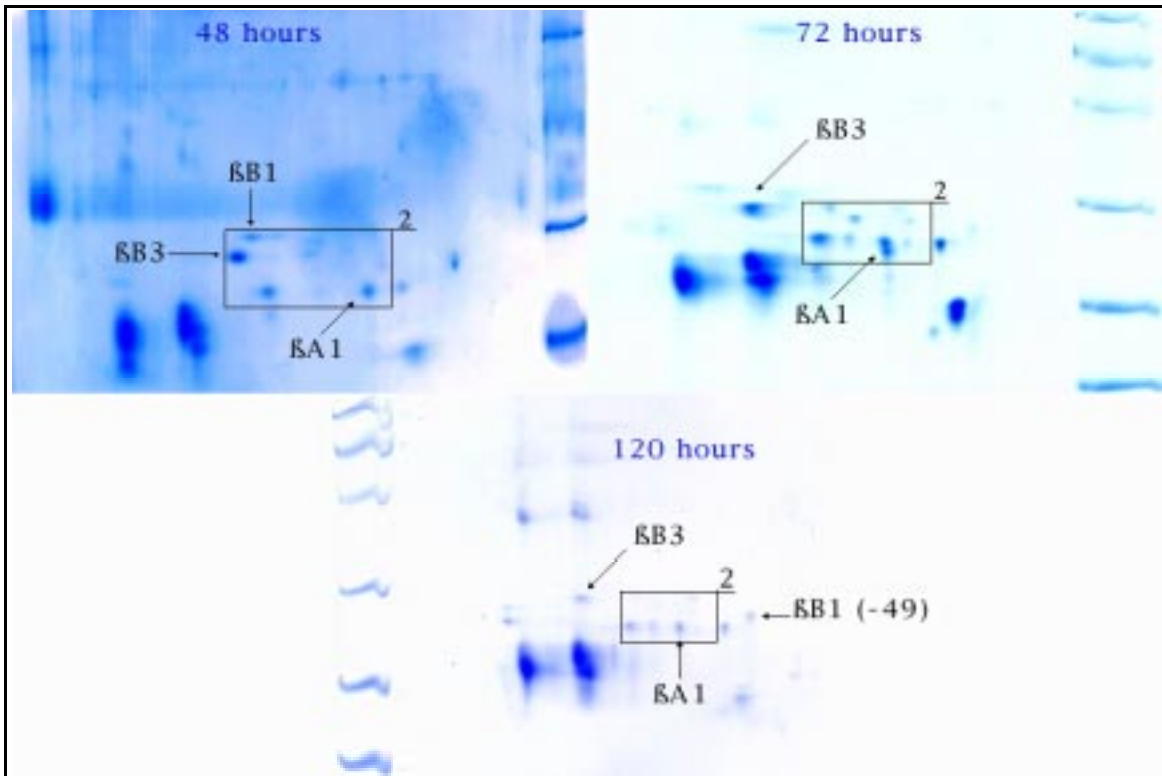
Figure 4-3 : Lens Nuclear Proteins 120 hours after Selenite

This trend in proteolysis is also apparent in box 1 of Figure 4-3, which represents the most acidic of the β -crystallins. In the gels from negative control lenses, one major protein (β A4) is seen, with one minor species, β B1 less an N-terminal peptide of 49 amino acids (β B1-49) also present in the urea

soluble fraction. For the buffer-soluble protein fraction from the Mn(III)-salophen/selenite treated lens, both β A4 and β B1-49 are also present, with the proteolyzed fragment β B1-49 at lower intensity than the native β A4 crystallin. Although the positive control appears to have the same fragments in the buffer-soluble fraction, the proteolyzed β B1-49 has the higher relative intensity. In the urea-soluble fractions, the Mn(III)-salophen/selenite-treated lenses had the greatest number of fragments over a larger pI range, possibly caused by deamidation or further proteolysis.

In the γ -crystallin region separations, the buffer-soluble protein fraction shows little difference between positive control, negative control, and Mn(III)-salophen/selenite treated lenses (Figure 4-3). An additional low-molecular weight basic species, probably a proteolytic product with a similar pI to its native form, is present in urea-soluble fractions from positive control lenses. Another difference is observed in the γ -crystallin region of the gel. In the Mn(III)-salophen/selenite treated lens, the majority of the γ -crystallin occurs with a lower molecular weight, indicating greater proteolysis not seen in the positive control fractions.

It was possible that Mn(III)-salophen interfered with the calpain-mediated proteolysis. To explore the extent of crystallin proteolysis in the presence of Mn(III)-salophen, we compared two-dimensional separations of buffer-soluble fractions from nuclear region of Mn(III)-salophen/selenite treated lenses 48, 72 and 120 hours after selenite injection (Figure 4-4).



2-D Gels of nuclear fractions from lenses of animals treated with Mn(III)-salophen and selenite. Proteins are mapped over a pH = 3-10 range (basic end is left on scans above) The region 2 boxed above represents a portion of the β -crystallins. More distinct species are present in the 72 hour fraction, indicating a progression of proteolysis over time.

Figure 4-4 : Proteolytic Progression in Mn-S/Selenite-treated Lenses

The α -crystallins undergo moderate proteolysis between 48 and 120 hours in Mn(III)-salophen/selenite treated lenses. Several species of β -crystallins also are degraded in Mn(III)-salophen/selenite treated lenses, as seen in box 2 on Figure 4-4. Of the species present in box 2, β B1 decreases in intensity as its proteolytic product β B1-49 appears near β A4 (box 1, Figure 4-3). Also, β A1 splits into two spots, one of slightly lower molecular weight. The β B3 crystallin disappears from box 2, reappearing as it migrates to a more basic position when it has lost a N-terminal peptide of ~10 amino acids (β B3-10). This spot remains at its basic position at 120 hours, but has less intensity, as it loses another N-terminal peptide of 7 amino acids and generates β B3-17.

Glutathione content of lenses

Total glutathione levels were quantified in lenses from animals in the following groups: selenite only, Mn(III)-acetate, salophen and low and high dose Mn(III)-salophen treatment. The GSH level dropped to less than 30% of control levels in all groups treated with sodium selenite. Neither Mn(III)-salophen or its individual synthetic components gave protection against GSH loss (Figure 4-5).

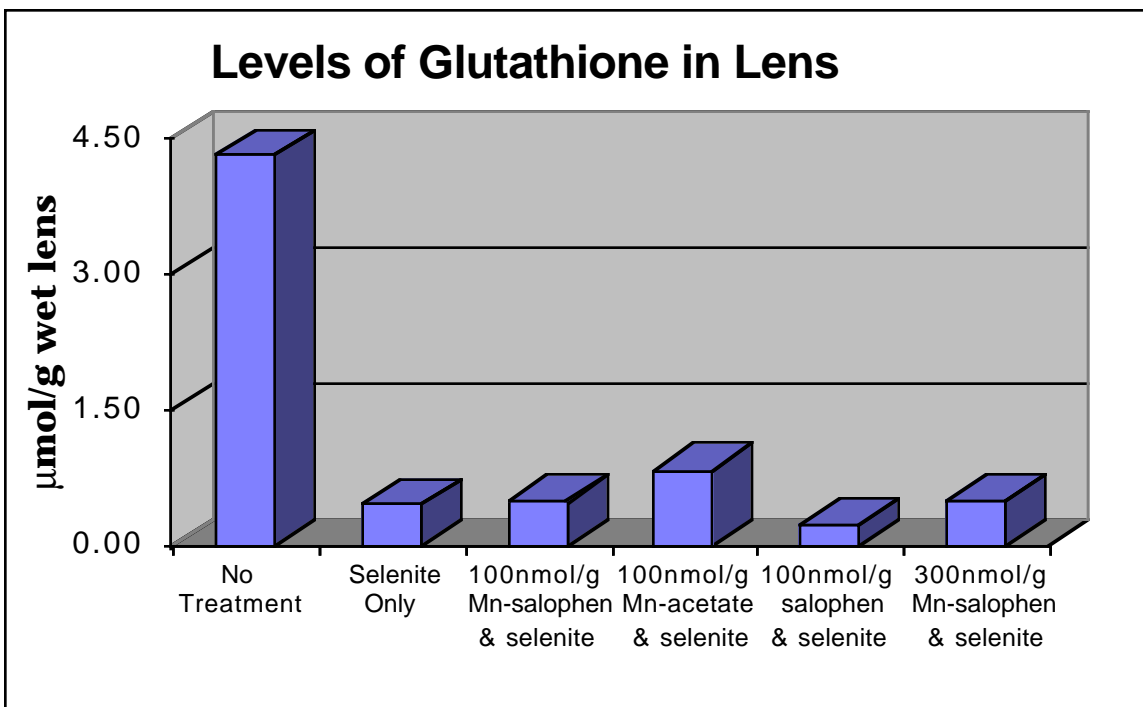


Figure 4-5 : Glutathione Levels after Mn(III)-salophen treatment

Elemental Analysis

Sodium, potassium and calcium levels were measured in lenses at 72 hours and 120 hours after selenite treatment. At 72 hours, visual protection cannot be conclusively determined, therefore all animals treated with both selenite and Mn(III)-salophen were grouped together. At 120 hours, nuclear transparency can be reproducibly evaluated under the dissecting microscope, and Mn(III)-salophen treated animals were separated into protected and unprotected categories.

Treatment with sodium selenite produced significant changes in elemental potassium and calcium at 72 hours. Calcium levels increased from 88 ppm to 137 parts per million and potassium decreased from 11.0 to 9.7 parts per thousand (Table 4-3). The trend in sulfur change, dropping from 12.2 to 11.6 parts per thousand, correlated with the drop in glutathione levels but was not statistically significant.

Table 4-3 : Elemental Analysis 72 Hours After Selenite Treatment

Mean values are reported as parts per thousand \pm Std Error unless otherwise noted, and were measured by ICP Spectroscopy from dried, acid-digested lens samples.

Group (N)	Ca ¹	K	Na	S
(-) controls (6)	87.5 \pm 13.0 ^a	10.95 \pm 0.34 ^a	2.55 \pm 0.30	12.17 \pm 0.29
Mn-salophen (4)	54.1 \pm 6.2 ^b	10.94 \pm 0.27 ^a	2.67 \pm 0.35	11.95 \pm 0.12
Mn-s/Selenite (5)	137.3 \pm 7.3 ^c	10.12 \pm 0.16 ^{a b}	2.67 \pm 0.33	11.57 \pm 0.14
(+) controls (5)	136.8 \pm 3.9 ^c	9.71 \pm 0.15 ^b	2.51 \pm 0.24	11.61 \pm 0.31

¹parts per million

^{a b c} Values designated with different letters are statistically different ($p < 0.05$)

At 72 hours after selenite treatment the calcium content was elevated ($p < 0.02$) compared to lenses from untreated animals. The decrease of potassium at 72 hours after selenite treatment was also significant ($p < 0.02$) Mn(III)-salophen did not preserve calcium or potassium homeostasis at 72 hours when given with selenite. ($p > 0.05$)

Table 4-4 : Elemental Analysis 120 hours after selenite treatment

Values are reported as parts per thousand \pm Std Error unless otherwise noted and were measured by ICP Spectroscopy from dried, acid-digested lens samples. Protected lenses and (-) controls had no nuclear opacity present. Unprotected lenses and (+) controls had dense nuclear opacities.

Group (N)	Ca ¹	K	Na	Na/K Ratio
(-) controls (16)	136.1 \pm 13.0 ^a	8.20 \pm 0.43 ^a	1.56 \pm 0.10 ^a	0.20
Protected Mn-s/Selenite (4)	165.8 \pm 4.8 ^b	6.78 \pm 0.17 ^b	4.37 \pm 0.20 ^b	0.64
Unprotected Mn-s/Selenite (10)	172.4 \pm 24.7 ^{a b}	8.01 \pm 0.42 ^a	2.27 \pm 0.13 ^c	0.28
(+) controls (8)	240.0 \pm 7.7 ^c	7.35 \pm 0.13 ^c	1.75 \pm 0.09 ^a	0.24

¹parts per million

^{a b c} Values designated with different letters are statistically different ($p < 0.05$)

After 120 hours, the difference in calcium levels between positive and negative controls was greater: 240 versus 136 parts per million respectively. (Table 4-4) These values are significantly different ($p < 0.05$). Treatment with

Mn(III)-salophen in addition to selenite resulted in a slightly higher level of calcium when compared to negative controls: 166 versus 136 parts per million respectively; however, these values were not significantly different. They were significantly different from the positive control level of 240 ($p < 0.03$). However, when calcium levels of protected lenses from animals treated with Mn(III)-salophen were compared to similarly treated animals without protection of lens transparency, no significant difference in calcium level was seen.

In Mn(III)-salophen-treated animals, sodium and potassium levels were affected 120 hours after selenite treatment. Sodium and potassium concentrations were similar in positive and negative control lenses. However, the lens sodium concentration increased dramatically in all Mn(III)-salophen-treated animals. Those lenses with nuclear cataracts had 50% increase in sodium, while protected lenses increased nearly 2-fold. The net effect is reflected by the increase in the sodium / potassium ratio.

Lens Water Content

Lenses from animals treated with selenite and Mn(III)-salophen had a dry to wet weight ratio of 33 ± 2 %, which was not different from either positive or negative control lenses.

Discussion

When considering the mechanism of visual protection by Mn(III)-salophen, several possibilities occur. First, Mn(III)-salophen could be preventing the delivery of selenite to the lens, either by directly reacting with it or by interfering with its transport. Second, Mn(III)-salophen could preserve calcium homeostasis, and thereby prevent calpain activation and its consequent proteolysis. Third, Mn(III)-salophen could alter the specific proteolytic course taken by the lens, either in rate or in direction. Finally, Mn(III)-salophen could interact directly with the crystallins, preventing aggregation of proteolyzed fragments into cataractous bodies.

Total Lens Protein and Nuclear / Cortical Distribution

The proteolytic events involved in selenite cataract are well known; however, the loss of total lens protein may result from either increased proteolysis or decreased synthesis. Because radioisotope labeling studies have shown a decrease in protein biosynthesis in response to glutathione depletion in the BSO model,²³ it is possible that both factors contribute to the net protein decrease. Regardless, the total lens protein can serve as an important marker of progress toward cataract.

The loss of lens protein in the lenses of Mn(III)-salophen/selenite treated animals is not consistent with our first hypothesis, interception of selenite prior to its toxic effect on the lens. Treatment with Mn(III)-salophen alone did not result in a loss of weight to the animal nor a loss of protein in the lens, so the effect seen in Mn(III)-salophen/selenite treated animals was caused by selenite treatment. The loss of protein, when combined with the observed

weight loss and the lenticular glutathione loss, ruled out the possibility of Mn(III)-salophen completely inactivating selenite.

Electrophoretic Studies

It is important to consider that when gels are normalized with the same amount of protein loaded, relative gel to gel comparisons can be misleading. For example, if the intensity of an arbitrary β -crystallin, βX , is lower in the urea-soluble fraction of Sample A when compared to the urea-soluble fraction of Sample B, then we may not conclude that more βX is present in Sample B unless Samples A and B have identical urea-soluble to buffer-soluble ratios. Due to these complicating factors, it is best to compare within similar sample groups.

The distribution of protein between nucleus and cortex is even more difficult to describe quantitatively. The boundary between the cortex and nucleus of the lens is a dynamic one, and treatment with sodium selenite alters the relative size of the nucleus. As the nuclear region opacifies, the spherical zone which separates it from the cortex shrinks until the nucleus is composed of entirely opaque tissue.

Those limitations aside, we can draw several important conclusions from our gel studies. First, there is a progression of proteolysis consistent with *m*-calpain activation in the nuclear, soluble β -crystallins of selenite-treated lenses, regardless of Mn(III)-salophen administration (Figure 4-4). Therefore, the increase in calcium concentration is sufficient to activate calpain. In a positive control lens we see significantly more distinct species of α -crystallins compared to negative controls. Upon detailed examination of lens total protein gels, the α -crystallin regions for negative controls and Mn(III)-salophen/selenite protected lenses appear identical. In contrast, the α -crystallin regions of unprotected and positive control lenses have significant proteolysis (Figure 4-2). Detailed examination of the nuclear region of positive control lenses reveals that the α -crystallin proteolytic pattern is essentially identical in the buffer and urea-soluble fractions, although the urea-soluble fraction appears to have more of the lower molecular-weight alpha fragments (Figure 4-3).

When combined with the observation that the α -crystallin region in the nuclear soluble fraction of Mn(III)-salophen protected lenses has much less degradation than that of positive control lenses, we conclude that Mn(III)-salophen protects α -crystallin structure *in vivo*. Such protection potentially could be effected by lowering the activity of *m*-calpain with Mn(III)-salophen treatment, which in turn could be due to maintenance of Ca^{2+} homeostasis.

Calcium Homeostasis

The calcium elevation in selenite-treated animals regardless of Mn(III)-salophen treatment is consistent with the observation of calpain-type proteolysis within the lens fractions. Although the trend toward greater calcium concentration at 72 hours in lenses from Mn(III)-salophen/selenite

treated animals and positive controls was not different, the 120 hour data show that the Mn(III)-salophen treatment protects the lens from further significant rises in calcium after 72 hours. The lack of correlation between the 72 and 120 hour data is not necessarily surprising, given that the nuclear opacification takes place after 72 hours while the calcium levels are still rising. One possible explanation for the less extensive proteolysis reported above is that Mn(III)-salophen simply preserves the calcium balance sufficiently that calpain-mediated proteolysis is less complete or not fast enough for cataract formation. The possibility of partial or differential activation of calpain has not been explored in this model, due to the overwhelming increase of calcium seen on positive control lenses.

Sodium/Potassium Homeostasis and Lens Hydration

The 10% decrease of potassium concentration at 72 hours (Table 4-3) is consistent with trends reported by Wang *et al.*,¹⁰² although they did not have a sufficiently distinct separation for statistical significance. This perturbation in potassium levels could be explained by several causes. It is consistent with an elevation of hydrogen peroxide within the lens, because hydrogen peroxide damages the Na⁺/K⁺ ATPase. Depletion of GSH in lens epithelial cells, which also occurs in lenses from animal treated with selenite, has been shown to cause inactivation of Na⁺/K⁺ ATPase⁴⁹. Given that the changes in potassium concentration seen at 72 hours are not different at 120 hours, it is possible that an early insult is recovering. In the selenite model, the posterior subcapsular opacity (PSO) is clearly seen by 24 hours but is rarely seen beyond 72 hours. It is possible that the initial oxidative burst caused by delivery of selenite to the posterior lens is the cause of the PSO. What would be large perturbations at the individual fiber cell could be very difficult to detect when considering the lens as a whole.

Given the protection against calcium elevation when treated with Mn(III)-salophen, the significant shift in the sodium / potassium ratio seen in protected lenses is particularly important. One explanation for the shift, which is caused primarily by sodium elevation, is an active cationic Na/Ca exchange. If Mn(III)-salophen localizes to peripheral lipids and stabilizes them against peroxidative damage, then the integral exchange protein could continue to compensate against Ca⁺⁺ influx. Of course, the sodium would have to be removed later, and an inability to do so could partially explain the long-term failure of Mn(III)-salophen to protect against cataract formation (Figure 2-6).

The overall hydration state of the lens is also important to consider. Undamaged adult lenses consist of approximately 67% (w/w) water, lower than many tissues in the body. Many forms of cataract involve changes in hydration, which can alter the refractile index and scatter light. At the stage of nuclear cataract, the selenite model does not involve significant hydration perturbations, so we did not expect to see any effect of Mn(III)-salophen with respect to hydration in this model. However, given the shift in ion ratios, it was important to establish that Mn(III)-salophen was innocuous in this respect. Our data showed no indication of changes in water content regardless of Mn(III)-salophen treatment.

Sulfur and Manganese Levels

In adult lenses, glutathione is the major source of sulfur; however, in neonatal lenses, the γ -crystallins are most significant. Because of the effect of selenite treatment upon glutathione levels, we investigated the effect of Mn(III)-salophen upon total sulfur in the lens. As no significant effect was seen at 72 hours after selenite injection, these studies were not continued at the 120 hour timepoint.

For technical reasons involving quantity of solvent necessary for assay, determining more than four elements would require diluting our samples or using more animals for tissue sources. When we eliminated sulfur from our necessary list, we added manganese in an attempt to determine any elevation corresponding to Mn(III)-salophen administration. An individual lens weighing ~15 mg did not show a manganese level above our detection threshold of 1 p.p.b. Lenses from animals given Mn(III)-salophen also did not have detectable levels of manganese (data not shown).

From this study it appears that overwhelming α -crystallin proteolysis is the seminal event in the protein aggregation involved in cataract formation. Activation of *m*-calpain, while necessary for cataract formation, is not itself sufficient if only extensive β -crystallin modifications occur.

We can speculate that the superoxide generated from selenite metabolism could damage the α -crystallins directly or that damage to the lipid membranes helps destabilize α -crystallins, reducing their chaperone function. The similarities between the Mn(III)-salophen protected lens's protein configuration at 72 hours after selenite and the positive control suggest that aggregation is mediated by factors beyond simple proteolysis and that repair or arrest of ongoing oxidative change can be accomplished by systemic treatment with antioxidants.

SUMMARY AND CONCLUSIONS

Visual Protection by Mn(III)-salophen

Administration of 300 $\mu\text{mol/kg}$ Mn(III)-salophen IP to neonatal rats provides significant short-term protection against nuclear cataract formation in the selenite model. The nucleus remains transparent, although slight cortical opacities remain. This treatment is limited to animals under 25 grams at the time of selenite injection, and is not effective if given SQ. The lenses from an animal maintained into adulthood are not protected, as the lenses develop diffuse opacities.

The cataract development seen in positive controls within litters treated with Mn(III)-salophen was distinctly less than that seen in positive controls from litters without Mn(III)-salophen present. This effect was attributed to cross-contamination of positive controls by their Mn(III)-salophen-treated littermates; however, this effect is not easily explained by transdermal absorption, given the significant reduction in efficacy of Mn(III)-salophen when given subcutaneously compared to intraperitoneally.

It is possible that hepatic metabolism is important and that a metabolite of Mn(III)-salophen may be the active species, but we have no direct evidence to support that possibility. If transformation forms a compound with higher biological activity, then the low concentrations of excreted products present in urine or feces could be responsible for the cross-contamination seen in the morphology and ion levels of positive control lenses from littermates treated with Mn(III)-salophen. It seems unlikely that such an excreted product would be readily absorbed, however. Regardless of etiology, the contamination issue was resolved by using age-matched positive controls from litters without Mn(III)-salophen.

DMSO was chosen as a vehicle because it is less toxic than other solvents capable of dissolving the hydrophobic Mn(III)-salophen. Mn(III)-acetate, while soluble in water, very rapidly disproportionates into Mn(II) and Mn(IV) species. By using DMSO it is possible that Mn(III)-salophen could partition directly into membrane lipids, though it seems unlikely that a charged species could be embedded completely.

If we consider the possibility of a peripheral membrane association, the compound may be serving to sequester active manganese in a particularly vulnerable location within the lens. Localization of metal ions near phosphate groups inside the cell is a well-known phenomenon. For example, free iron and the negatively charged phosphate backbone of DNA associate readily, predisposing DNA to hydroxyl radical-mediated damage formed by the metal-catalyzed Haber-Weiss reaction.

If we extend that localization concept to manganese, the salophen ligand may serve as a carrier, protecting the biologically active Mn ion from water until it reaches its destination. The partial protection against unregulated

calcium influx could be due to protection of lipid membranes from peroxidation by Mn(III)-salophen. The rigidity of lens membranes makes them particularly prone to leakage from conformational shearing; therefore, even mild peroxidation could cause significant ionic disturbances. This hypothesis is consistent with our observations that Mn(III)-acetate has similar though smaller magnitude effects to Mn(III)-salophen both *in vitro* and *in vivo* as well as reports of Mn(III)-acetate being shown to have superoxide scavenging effects when in solution with macromolecules which can sequester it from water.⁶⁷

The extent of delivery of Mn(III)-salophen to the lens is currently unclear. As Mn(III)-salophen does not protect against glutathione loss or calpain-mediated proteolysis, we may conclude that the complex is not intercepting selenite prior to its effect on the lens. A definitive resolution of the pharmacology of Mn(III)-salophen would require radiolabeling with either ⁵⁴Mn or ¹⁵N for the synthetic components Mn(III)-acetate or salophen respectively. That experiment poses considerable risk to laboratory personnel due to the absorptivity of DMSO, and the dangers of radioisotope contamination.

In vitro GSH/Selenite Reaction

Mn(III)-salophen significantly preserves the lifetime of GSSeSG at the cost of lower GSH in the GSH-mediated reduction of selenite. The observed persistence of GSSeSG was not replicated when superoxide dismutase (SOD) or catalase replaced Mn(III)-salophen, but was preserved with DMPO. No radical-DMPO adduct was detected by EPR. A partial preservation of GSSeSG was seen when Mn(III)-acetate was used in place of DMPO or Mn(III)-salophen. A similar preservation has been seen previously in our laboratory using the generic electron acceptor nitroblue tetrazolium (NBT). (Hess and Smith, unpublished data)

When combined with the observation that GSH is not consumed in the breakdown of GSSeSG, these data suggest the presence of another electron donor generated during the GSH/selenite reaction. This other species is responsible for the reduction of GSSeSG to selenide and subsequent generation of superoxide. By intercepting this species, Mn(III)-salophen can delay the oxidative burst associated with selenite administration.

The absence of a long-term protective effect of Mn(III)-salophen is disappointing, but neither unexpected nor unreasonable in light of our proposed mechanism. If the Mn(III)-salophen complex effectively sequesters selenodiglutathione by temporary removal of ROS, then endogenous oxidative stress from normal metabolic processes could slowly overwhelm that protection over a longer period of time. Because the lens presumably does not have a mechanism for export of GSSeSG, it would remain in the lens until metabolized, at which time it could incite further oxidative damage.

Calcium / Ion homeostasis

Mn(III)-salophen provides an intermediate level of protection against loss of calcium homeostasis 120 hours after selenite treatment. A moderate reduction of *m*-calpain activity secondary to lower calcium levels could be the cause of alpha-crystallin protection. The impact of loss of calcium homeostasis is most profound in the nucleus, since that region of the lens does not have Ca-ATPase activity.¹³ Another significant consequence of Mn(III)-salophen protection is a 2-fold increase of the sodium / potassium ratio, which could contribute to both the mechanism for protection of calcium homeostasis and the long-term derangement of the lens.

Crystallin Proteolysis

Mn(III)-salophen treatment does not impair *m*-calpain type proteolysis of β -crystallins within the nucleus, although some protection is seen for the α -crystallins. Overall, the differences are slight between Mn(III)-salophen treated lenses which were protected against cataract formation and those which were not. The urea-soluble nuclear fraction from animals protected by Mn(III)-salophen showed many more post-translationally modified proteins than were evident in either positive or negative controls. Therefore Mn(III)-salophen does not protect against cataract solely by inhibiting proteolysis.

The observation that cysteine protease inhibitors arrest the cataractogenic pathway implies a causal relationship between proteolysis and cataract; however, our finding that similar proteolytic patterns may be obtained without visual opacity demonstrates that proteolysis, while necessary, is not sufficient for cataract formation. Based on our findings in the gel electrophoresis studies, β -crystallin proteolysis may proceed without visual opacity provided the chaperone function of α -crystallin remains intact. Because α -crystallin acts to stabilize proteins in early stages of unfolding rather than early folding during synthesis, it is well-suited for the role we describe.

Model for in vivo protection with Mn(III)-salophen

Our data are consistent with the following model of Mn(III)-salophen *in vivo*: Mn(III)-salophen, after IP injection, enters the portal circulation and is transformed by the liver into an unknown metabolite. That metabolite travels through the circulatory system until it reaches the lens, where it enters by diffusion through the neonatal vascular bed. Once present, it interferes with the metabolism of selenite after the initial glutathione drop by preventing the breakdown of selenodiglutathione. This interference alters the lens response to ionic disturbances and partially protects alpha-crystallin structure. The overall preservation of the lens is sufficient to overcome the initial insult for short-term visual protection; however, the protection does not last into adulthood.

LITERATURE CITED

- ¹Anderson, R. S., Shearer, T. R., & Claycomb, C. K. (1986) Selenite-induced epithelial damage and cortical cataract, *Curr Eye Res* **5**, 53-61.
- ²Andley, U. P., Mathur, S., Griest, T. A., & Petrash, J. M. (1996) Cloning, expression, and chaperone-like activity of human alphaA-crystallin, *J Biol Chem* **271**, 31973-31980.
- ³Ansari, N. H., & Srivastava, S. K. (1983) Role of glutathione in the prevention of cataractogenesis in rat lenses, *Curr Eye Res* **2**, 271-275.
- ⁴Azuma, M., Fukiage, C., David, L. L., & Shearer, T. R. (1997) Activation of Calpain in Lens: A Review and Proposed Mechanism, *Exp Eye Res* **64**, 529-538.
- ⁵Babizhayev, M. A., Deyev, A. I., & Linberg, L. F. (1988) Lipid Peroxidation as a Possible Cause of Cataract, *Mechanisms of Ageing and Development* **44**, 69-89.
- ⁶Benedek, G. B. (1971) Theory of Transparency of the Eye, *Applied Optics* **10**, 459-473.
- ⁷Bernardini, G., & Peracchia, C. (1981) Gap junction crystallization in lens fibers after an increase in cell calcium, *Invest Ophthalmol Vis Sci* **21**, 291-299.
- ⁸Bhatnagar, A., Ansari, N. H., Wang, L., Khanna, P., Wang, C., & Srivastava, S. K. (1995) Calcium-Mediated Disintegrative Globulization of isolated Ocular Lens Fibers Mimics Cataractogenesis, *Exp Eye Res* **61**, 303-310.
- ⁹Bhuyan, K. C., Bhuyan, D. K., Chiu, W., Malik, S., & Freidovich, I. (1991) Mn(III)-desferal in therapy of diquat-induced cataract in rabbit, *Arch Biochem Biophys* **288**, 525-532.
- ¹⁰Bindels, J. G., Bours, J., & Hoenders, H. J. (1983) Age-Dependent Variations in the Distributions of Rat Lens Water-Soluble Crystallins. Size Fractionation and Molecular Weight Determination, *Mechanisms of Ageing and Development* **21**, 1-13.
- ¹¹Bjornstedt, M., Kumar, S., & Holmgren, A. (1992) Selenodiglutathione Is a Highly Efficient Oxidant of Reduced Thioredoxin and a Substrate for Mammalian Thioredoxin Reductase, *J Biol Chem* **267**, 8030-8034.
- ¹²Bjornstedt, M., Odlander, B., Kuprin, S., Claesson, H. E., & Holmgren, A. (1996) Selenite Incubated With NADPH and Mammalian Thioredoxin Reductase Yields Selenide, Which Inhibits Lipoygenase and Changes the Electron Spin Resonance Spectrum Of the Active Site Iron, *Biochemistry* **35**, 8511-8516.

- ¹³Borchman, D., Delamere, N. A., & Paterson, C. A. (1988) Ca-ATPase Activity in the Rabbit and Bovine Lens, *Invest Ophthalmol Vis Sci* **29**, 982-987.
- ¹⁴Bours, J., & Hockwin, O. (1983) Biochemistry of the Ageing Rat Lens, *Ophthalmic Res* **15**, 234-239.
- ¹⁵Boyle, D. L., Blunt, D. S., & Takemoto, L. J. (1997) Confocal Microscopy of Cataracts from Animal Model Systems: Relevance to Human Nuclear Cataract, *Exp Eye Res* **64**, 565-572.
- ¹⁶Bradford, M. M. (1976) A rapid and sensitive method for the quantitation of microgram quantities of protein utilizing the principle of protein dye binding., *Anal Biochem* **72**, 248-254.
- ¹⁷Braugher, J. M., Duncan, L. A., & Chase, R. L. (1986) The Involvement of Iron in Lipid Peroxidation, *J Biol Chem* **261**, 10282-10289.
- ¹⁸Brehe, J. E., & Burche, H. B. (1976) Enzymatic Assays for Glutathione, *Anal Biochem* **71**, 189-197.
- ¹⁹Bunce, G. E., & Hess, J. L. (1981) Biochemical Changes Associated with Selenite-induced Cataract in the Rat, *Exp Eye Res* **33**, 505-514.
- ²⁰Bunce, G. E., Hess, J. L., & Batra, R. (1984) Lens calcium and selenite-induced cataract, *Curr Eye Res* **3**, 315-320.
- ²¹Burk, R. F. (1991) Molecular biology of selenium with implications for its metabolism, *FASEB J* **5**, 2274-2278.
- ²²Calvin, H. I., Medvedosvsky, C., & Worgul, B. V. (1986) Near-total glutathione depletion and age-specific cataracts induced by buthione sulfoximine in mice, *Science* **233**, 553-555.
- ²³Calvin, H. I., Wu, J.-X., Viswanadhan, K., & Fu, S.-C. J. (1996) Modifications in Lens Protein Biosynthesis Signal the Initiation of Cataracts Induced by Buthione Sulfoximine in Mice, *Exp Eye Res* **63**, 357-368.
- ²⁴Carver, J. A., Nicholls, K. A., Aquilina, J. A., & Truscott, R. J. W. (1996) Age-related Changes in Bovine α -crystallin and High-molecular-weight Protein, *Exp Eye Res* **63**, 639-647.
- ²⁵Christen, W. G., Glynn, R. J., & Hennekens, C. H. (1996) Antioxidants and Age Related Eye Disease: Current and Future Perspectives, *Annals Of Epidemiology Jan* **6**, 60-66.
- ²⁶Clark, J. I., Danford-Kaplan, M. E., & Delaye, M. (1988) Calcium Decreases Transparency of Homogenate from Lens Cortex and has no Effect on Nucleus, *Exp Eye Res* **47**, 447-455.

- ²⁷Clark, J. I., & Huang, Q.-L. (1996) Modulation of the chaperone-like activity of bovine α -crystallin, *Proc Natl Acad Sci USA* **93**, 15185-15189.
- ²⁸Clark, J. I., Livesey, J. C., & Steele, J. E. (1996) Delay or Inhibition of Rat Lens Opacification using Pantethine and WR-77913, *Exp Eye Res* **62**, 75-84.
- ²⁹Clark, J. I., & Steele, J. E. (1992) Phase-separation inhibitors and prevention of selenite cataract, *Proc Natl Acad Sci USA* **89**, 1720-1724.
- ³⁰Cui, X.-L., & Lou, M. F. (1993) The effect and recovery of long-term H₂O₂ exposure on lens morphology and biochemistry, *Exp Eye Res* **57**, 157-167.
- ³¹David, L. L., Azuma, M., & Shearer, T. R. (1994) Cataract and the acceleration of calpain-induced beta-crystallin insolubilization occurring during normal maturation of rat lens, *Invest Ophthalmol Vis Sci* **35**, 785-793.
- ³²David, L. L., & Shearer, T. R. (1984) Calcium-Activated Proteolysis in the Lens Nucleus during Selenite Cataractogenesis, *Invest Ophthalmol Vis Sci* **25**, 1275-1283.
- ³³David, L. L., & Shearer, T. R. (1984) State of Sulfhydryl in Selenite Cataract, *Toxicol Appl Pharmacol* **74**, 109-115.
- ³⁴David, L. L., & Shearer, T. R. (1993) β -Crystallins insolubilized by calpain II in vitro contain cleavage sites similar to β -crystallins insolubilized during cataract, *FEBS Letters* **324**, 265-270.
- ³⁵Davis, R. L., & Spallholz, J. E. (1996) Inhibition of Selenite-Catalyzed Superoxide Generation and Formation of Elemental Selenium (Se⁰) by Copper, Zinc, and Aurintricarboxylic Acid (ATA), *Biochem Pharmacol* **51**, 1015-1020.
- ³⁶Day, B. J., Fridovich, I., & Crapo, J. D. (1997) Manganic Porphyrins Possess Catalase Activity and Protect Endothelial Cells against Hydrogen Peroxide-Mediated Injury, *Arch Biochem Biophys* **347**, 256-262.
- ³⁷Delamere, N. A., Paterson, C. A., & Hensley, S. (1988) Lens Membrane Properties Following Hydrogen Peroxide Exposure, *Ophthalmic Res* **20**, 200-204.
- ³⁸Delaye, M., & Tardieu, A. (1983) Short-range order of crystallin proteins accounts for eye lens transparency, *Nature* **302**, 415-417.
- ³⁹Deneke, S. M., & Fanburg, B. L. (1989) Regulation of cellular glutathione, *Am J Physiol* **257**, L163-L173.
- ⁴⁰Denko, C. W., Goodman, R. M., Miller, R., & Donovan, T. (1967) Distribution of Dimethyl Sulfoxide-³⁵S in the Rat, *Ann NY Acad Sci* **141**, 77-84.

- ⁴¹Devamanoharan, P. S., Henein, M., Morris, S., Ramachandran, S., Richards, R. D., & Varma, S. (1991) Prevention of selenite cataract by vitamin C, *Exp Eye Res* **52**, 563-568.
- ⁴²Frederikse, P. H., Garland, D., Zigler, J. S., & Piatigorsky, J. (1996) Oxidative Stress Increases Production of β -Amyloid Precursor Protein and β -Amyloid (A β) in Mammalian Lenses, and A β Has Toxic Effects on Lens Epithelial Cells, *J Biol Chem* **271**, 10169-10174.
- ⁴³Fridovich, I. (1986) Biological Effects of the Superoxide Radical, *Arch Biochem Biophys* **247**, 1-11.
- ⁴⁴Fridovich, I. (1989) Superoxide Dismutases: An Adaptation to a Paramagnetic Gas, *J Biol Chem* **264**, 7761-7764.
- ⁴⁵Fridovich, I. (1995) in *Annual Review of Biochemistry* (Richardson, C. C., Abelson, J. N., Meister, A., & Walsh, C. T., Eds.) pp 91-112, Annual Reviews Inc., Palo Alto, CA.
- ⁴⁶Fridovich, I. (1997) Superoxide anion radical (O₂⁻), superoxide dismutases, and related matters, *J Biol Chem* **272**, 18515-18517.
- ⁴⁷Gallagher, S. R., & Smith, J. A. (1996) in *Current Protocols in Molecular Biology* (Ausubel, F. M., Brent, R., Kingston, R. E., Moore, D. D., Seidman, J. G., Smith, J. A., & Struhl, K., Eds.) pp 10.12.11-10.12.21, John Wiley and Sons, New York.
- ⁴⁸Ganea, E., & Harding, J. J. (1996) Inhibition of 6-Phosphogluconate Dehydrogenase by Carbamylation and Protection by α -crystallin, a Chaperone-like Protein, *Biochem Biophys Res Comm* **222**, 626-631.
- ⁴⁹Giblin, F. J., Chakrapani, B., & Reddy, V. N. (1976) Glutathione and lens epithelial function, *Invest Ophthalmol Vis Sci* **15**, 381-393.
- ⁵⁰Giblin, F. J., & McCready, J. P. (1983) The Effect of Inhibition of Glutathione Reductase on the Detoxification of H₂O₂ by Rabbit Lens, *Invest Ophthalmol Vis Sci* **24**, 113-118.
- ⁵¹Giblin, F. J., McCready, J. P., Schrimsher, L., & Reddy, V. N. (1987) Peroxide-induced Effects on Lens Cation Transport Following Inhibition of Glutathione Reductase Activity In Vitro, *Exp Eye Res* **45**, 77-91.
- ⁵²Green, K. (1995) Free radicals and aging of anterior segment tissues of the eye: a hypothesis, *Ophthalmic Res* **27 Suppl 1**, 143-149.
- ⁵³Green, M. J., & Hill, H. A. O. (1984) in *Methods in Enzymology* (Packer, L., Ed.) pp 3-21, Academic Press, Orlando.

- ⁵⁴Halliwell, B., & Aruoma, O. I. (1991) DNA Damage by oxygen-derived species, *FEBS Letters* **281**, 9-19.
- ⁵⁵Halliwell, B., & Gutteridge, J. M. (1990) Role of Free Radicals and Catalytic Metal Ions in Human Disease: An Overview, *Methods in Enzymology* **186**, 1-45.
- ⁵⁶Harman, L. S., Carver, D. K., Schreiber, J., & Mason, R. P. (1986) One- and Two-electron Oxidation of Reduced Glutathione by Peroxidases, *J Biol Chem* **261**, 1642-1648.
- ⁵⁷Harman, L. S., Mottley, C., & Mason, R. P. (1984) Free Radical Metabolites of L-Cysteine Oxidation, *J Biol Chem* **259**, 5606-5611.
- ⁵⁸Henle, E. S., & Linn, S. (1997) Formation, Prevention, and Repair of DNA Damage by Iron/Hydrogen Peroxide, *J Biol Chem* **272**, 19095-19098.
- ⁵⁹Hess, J. L., Mitton, K. P., & Rathbun, W. B. (1996) Impact of Methyl Thiazolidine Carboxylic Acid on Selenite-Induced Cataract, *Invest Ophthalmol Vis Sci* **37**, (Supplement, Abstract 972).
- ⁶⁰Hightower, K. R., Reddan, J. R., & Dziejcz, D. C. (1989) Susceptibility of Lens Epithelial Membrane SH Groups to Hydrogen Peroxide, *Invest Ophthalmol Vis Sci* **30**, 569-574.
- ⁶¹Hiraoka, T., Clark, J. I., Li, X. Y., & Thurston, G. M. (1996) Effect of selected anti-cataract agents on opacification in the selenite cataract model, *Exp Eye Res* **62**, 11-19.
- ⁶²Hoefer. (1992) , Hoefer Scientific Instruments.
- ⁶³Huang, L. L., Hess, J. L., & Bunce, G. E. (1989) Protection against cataract formation by antioxidants in rats receiving chronic, low doses of selenite, *Invest Ophthalmol Vis Sci* **30**, 330.
- ⁶⁴Jahngen-Hodge, J., Obin, M. S., Gong, X., Shang, F., Nowell, T. R. J., Gong, J., Abasi, H., Blumberg, J., & Taylor, A. (1997) Regulation of Ubiquitin-conjugating Enzymes by Glutathione Following Oxidative Stress, *J Biol Chem* **272**, 28218-28226.
- ⁶⁵Kelley, M. J., David, L. L., Iwasaki, N., Wright, J., & Shearer, T. R. (1993) Alpha-Crystallin Chaperone Activity Is Reduced by Calpain II *in Vitro* and in Selenite Cataract, *J Biol Chem* **268**, 18844-18849.
- ⁶⁶Kim, I. Y., & Stadtman, T. C. (1997) Inhibition of NF- κ B DNA binding and nitric oxide induction in human T cells and lung adenocarcinoma cells by selenite treatment, *Proc Natl Acad Sci USA* **94**, 12904-12907.

- ⁶⁷Kittiponkul, V. (1996) Effect of Oxidative Stress on *Escherichia coli* *sodA-sodB*:- Protection by the Mimic of Superoxide Dismutase, Mn(III)-salophen, *MS Thesis, VPISU Dept of Biochemistry*.
- ⁶⁸Klintworth, G. K., & Garner, A. (1994) in *Pathobiology of Ocular Disease, a Dynamic Approach* (Klintworth, G. K., & Garner, A., Eds.) pp 481-531, Marcel Dekker, Inc, New York.
- ⁶⁹Kramer, G. F., & Ames, B. N. (1988) Mechanisms of mutagenicity and toxicity of sodium selenite (Na₂SeO₃) in *Salmonella typhimurium*, *Mutat Res* **201**, 169-180.
- ⁷⁰Lanfear, J., Fleming, J., Wu, L., Webster, G., & Harrison, P. R. (1994) The selenium metabolite selenodiglutathione induces p53 and apoptosis: relevance to the chemoprotective effects of selenium?, *Carcinogenesis* **15**, 1387-1392.
- ⁷¹Lerman, S., & Borkman, R. F. (1979) A molecular model of lens aging, nuclear and cortical cataract formation, *Metab Pediat Ophthal* **3**, 27-35.
- ⁷²Liu, Z.-X., Robinson, G. R., & Gregory, E. M. (1994) Preparation and characterization of Mn-salophen complex with superoxide scavenging activity, *Arch Biochem Biophys* **315**, 74-81.
- ⁷³Lou, M. F., Dickerson, J. E., Jr, & Garadi, R. (1990) The Role of Protein-Thiol Mixed Disulfides in Cataractogenesis, *Exp Eye Res* **50**, 819-826.
- ⁷⁴Lund, A. L., Smith, J. B., & Smith, D. L. (1996) Modifications of the Water-insoluble Human Lens α -Crystallins, *Exp Eye Res* **63**, 661-672.
- ⁷⁵Maitra, I., Serbinova, E., Trischler, H., & Packer, L. (1995) Alpha-lipoic acid prevents buthionine sulfoximine-induced cataract formation in newborn rats, *Free Radic Biol Med* **18**, 823-829.
- ⁷⁶Matsushita, T., & Shono, T. (1981) Reactions of Manganese(III) Schiff Base Complexes with Superoxide Ion in Dimethyl Sulfoxide, *Bulletin of the Chemical Society of Japan* **54**, 3743-3748.
- ⁷⁷McCord, J. M., & Fridovich, I. (1969) Superoxide dismutase: an enzymatic function for erythrocyte, *J Biol Chem* **244**, 6049-6055.
- ⁷⁸Michiels, C., Raes, M., Toussaint, O., & Remacle, J. (1994) Importance of Se-Glutathione Peroxidase, Catalase, and Cu/Zn SOD for Cell Survival Against Oxidative Stress, *Free Radical Biology and Medicine* **17**, 235-248.
- ⁷⁹Misra, H. P. (1974) Generation of Superoxide Free Radical during the Autoxidation of Thiols, *J Biol Chem* **249**, 2151-2155.

⁸⁰Mitton, K. P., Bunce, G. E., & Hess, J. L. (1997) Free Amino Acids Reflect Impact of Selenite-Dependent Oxidation Stress on Primary Metabolism in Rat Lens, *Curr Eye Res* **16**, 997-1005.

⁸¹Moxon, A. L., & Rhian, M. (1943) Selenium Poisoning, *Physiological Reviews* **23**, 305-337.

⁸²Nakagawa, T., Aoyama, E., Kobayashi, N., Tanaka, H., Chikuma, M., Sakurai, H., & Nakayama, M. (1988) Thiol Exchange Reactions involving Selenotrisulfides, *Biochem Biophys Res Comm* **150**, 1149-1154.

⁸³Ohtsu, A., Kitahara, S., & Fujii, K. (1986) Anticataract properties of γ -glutamylcysteine ethyl ester in an animal model of cataract., *Ophthalmic Res* **18**, 236-242.

⁸⁴Oude Elferink, R. P. J., Ottenhoff, R., Liefting, W. G. M., Schoemaker, B., Groen, A. K., & Jansen, P. L. M. (1990) ATP-dependent efflux of GSSG and GS-conjugate from isolated rat hepatocytes, *Am J Physiol* **258**, G699-G706.

⁸⁵Paterson, C. A., & Delamere, N. A. (1992) in *Adler's Physiology of the Eye* (Hart, W. M., Ed.) pp 348-390, Mosby, St. Louis, MO.

⁸⁶Raman, B., & Rao, C. M. (1994) Chaperone-like Activity and Quaternary Structure of α -crystallin, *J Biol Chem* **269**, 27264-27268.

⁸⁷Rao, N. A., Thaete, L. G., Delmage, J. M., & Sevanian, A. (1985) Superoxide Dismutase in Ocular Structures, *Invest Ophthalmol Vis Sci* **26**, 1778-1781.

⁸⁸Roberts, J. C., & Francetic, D. J. (1991) Time course for the elevation of glutathione in numerous organs of L1210-bearing CDF1 mice given the L-cysteine prodrug, RibCys, *Toxicology Letters* **59**, 245-251.

⁸⁹Ross, D., Mehlhorn, R. J., Moldeus, P., & Smith, M. T. (1985) Metabolism of Diethylstilbestrol by Horseradish Peroxidase and Prostaglandin-H Synthase, *J Biol Chem* **260**, 16210-16214.

⁹⁰Salem, I. A., & Amer, S. A. (1995) Kinetics and mechanism of the homogeneous reaction between some manganese(III)-Schiff base complexes and hydrogen peroxide in aqueous and sodium dodecyl sulphate solutions, *Transition Met Chem* **20**, 494-497.

⁹¹Shearer, T. R., David, L. L., & Anderson, R. S. (1987) Selenite Cataract: a review, *Curr Eye Res* **6**, 289-300.

⁹²Shearer, T. R., Shih, M., Azuma, M., & David, L. L. (1995) Precipitation of crystallins from young rat lens by endogenous calpain, *Exp Eye Res* **61**, 141-150.

- ⁹³Siezen, R. J., Wu, E., Kaplan, E. D., Thomson, J. A., & Benedek, G. B. (1988) Rat Lens γ -Crystallins, *J Mol Biol* **199**, 475-490.
- ⁹⁴Smulders, R. H. P. H., Carver, J. A., Lindner, R. A., van Boekel, M. A. M., Bloemendal, H., & de Jong, W. W. (1996) Immobilization of the C-terminal Extension of Bovine α A-Crystallin Reduces Chaperone-like Activity, *J Biol Chem* **271**, 29060-29066.
- ⁹⁵Spallholz, J. (1993) On the Nature of Selenium Toxicity and Carcinostatic Activity, *Free Rad Biol Med* **17**, 45-64.
- ⁹⁶Spector, A., Huang, R.-R. C., Wang, G.-M., Schmidt, C., Yan, G.-Z., & Chifflet, S. (1987) Does Elevated Glutathione Protect the Cell from H₂O₂ Insult?, *Exp Eye Res* **45**, 453-465.
- ⁹⁷Steiner, M. G., & Babbs, C. F. (1990) Quantitation of the Hydroxyl Radical by Reaction with Dimethyl Sulfoxide, *Arch Biochem Biophys* **278**, 478-481.
- ⁹⁸Sun, T.-X., Das, B. K., & Liang, J. J.-N. (1997) Conformational and Functional Differences between Recombinant Human Lens α A- and α B-Crystallin, *J Biol Chem* **272**, 6220-6225.
- ⁹⁹Török, Z., Horváth, I., Goloubinoff, P., Kovács, E., Glatz, A., Balogh, G., & Vigh, L. (1997) Evidence for a lipochaperonin: Association of active protein-folding GroESL oligomers with lipids can stabilize membranes under heat shock conditions, *Proc Natl Acad Sci USA* **94**, 2192-2197.
- ¹⁰⁰Wang, G. M., Raghavachari, N., & Lou, M. F. (1997) Relationship of protein-glutathione mixed disulfide and thioltransferase in H₂O₂-induced cataract in cultured pig lens, *Exp Eye Res* **64**, 693-700.
- ¹⁰¹Wang, Z., Hess, J. L., & Bunce, G. E. (1992) Calcium efflux in rat lens: Na/Ca-exchange related to cataract induced by selenite, *Curr Eye Res* **11**, 625-632.
- ¹⁰²Wang, Z., Hess, J. L., & Bunce, G. E. (1992) Deferoxamine Effect on Selenite-Induced Cataract Formation in Rats, *Invest Ophthalmol Vis Sci* **33**, 2511-2519.
- ¹⁰³Wilber, C. G. (1980) Toxicology of Selenium: A Review, *Clin Tox* **17**, 171-230.
- ¹⁰⁴Wistow, G. J., & Piatigorsky, J. (1988) Lens Crystallins: The Evolution and Expression of Proteins for a Highly Specialized Tissue, *Annu Rev Biochem* **57**, 479-504.
- ¹⁰⁵Yan, L., & Spallholz, J. E. (1993) Generation of Reactive Oxygen Species from the Reaction of Selenium Compounds with Thiols and Mammary Tumor Cells, *Biochem Pharm* **45**, 429-437.

¹⁰⁶Zigler, J. S., & Goosey, J. (1981) Aging of protein molecules: lens crystallins as a model system, *Trends in Biochemical Sciences* **6**, 133-136.

VITA

Kevin Dell was born in Patuxant River, Maryland on July 3, 1969. The son of a naval officer, he lived in many parts of the United States as well as overseas. He graduated from Episcopal High School in 1987 and matriculated to The College of William and Mary that fall. While an undergraduate, he participated in research involving the magnetic properties of spin-glass compounds under Dr. Gary C. DeFotis. He graduated in 1991 with a Bachelor of Science degree, majoring in Chemistry and minoring in Computer Science.

He married Lauren Elizabeth Yolken on January 9, 1993, and they moved to Blacksburg, Virginia where she attended veterinary school. After working for 18 months as a computer programmer, he entered graduate school in the Department of Biochemistry at Virginia Tech in January 1995. After his first year of graduate school, he began working with Dr. John Hess on the use of Mn(III)-salophen in the selenite cataract model.

He presented his findings at the annual meetings of the American Society for Biochemistry and Molecular Biology (ASBMB) and the Association for Research in Vision and Ophthalmology (ARVO) in 1996 and 1997 respectively. He is a recipient of a National Eye Institute Travel Fellowship for ARVO 1998. He completed the requirements for the Ph.D. in Biochemistry in 1998 and will attend medical school, preparing for a career in academic medicine.